IEEE Access
Multidisciplinary | Rapid Review | Open Access Journal

Received June 3, 2021, accepted June 29, 2021, date of publication July 5, 2021, date of current version July 16, 2021.

Digital Object Identifier 10.1109/ACCESS.2021.3094560

Compensation of Transmitter IQ Imbalance in Multi-User Hybrid Beamforming Systems

RACHIT MAHENDRA[1], (Graduate Student Member, IEEE), SAIF KHAN MOHAMMED[1,2], (Senior Member, IEEE), AND RANJAN K. MALLIK[1,2], (Fellow, IEEE)

[1]Department of Electrical Engineering, Indian Institute of Technology Delhi, New Delhi 110016, India
[2]Bharti School of Telecommunication Technology and Management (BSTTM), Indian Institute of Technology Delhi, New Delhi 110016, India

Corresponding author: Rachit Mahendra (rachit1207@gmail.com)

The work of Saif Khan Mohammed was supported by the Prof. Kishan Gupta and Pramila Gupta Chair at IIT Delhi. The work of Ranjan K. Mallik was supported in part by the Science and Engineering Research Board, a Statutory Body of the Department of Science and Technology, Government of India, under the J. C. Bose Fellowship.

ABSTRACT In this paper, we consider the uplink (UL) communication of a massive multi-user (MU) multiple-input multiple-output (MIMO) hybrid beamforming system (HBFS) in which the transmitting user-equipments are affected by IQ imbalance (IQI). We first show that if the transmitter IQI is not compensated, it will result in a finite ceiling of the UL achievable sum-rate at high signal-to-noise ratio, which only depends on the transmitter IQI matrices and is independent of the propagation channel and the choice of the hybrid combining matrices. This justifies the need for transmitter IQI compensation in massive MU-MIMO HBFS. Therefore, we propose a novel zero-forcing based transmitter IQI compensation algorithm to be implemented at the base station which effectively mitigates the undesired effects of transmitter IQI and is applicable for any channel model and any choice of the number of RF chains. For uncorrelated Rayleigh fading channel, we derive an approximate closed-form expression of the UL sum-rate achieved by the massive MU-MIMO HBFS with the proposed transmitter IQI compensation. Finally, numerical results are presented which confirm the effectiveness of the proposed transmitter IQI compensation algorithm in mitigating the undesired effects of transmitter IQI in different channel environments.

INDEX TERMS Amplitude and phase mismatch, hybrid beamforming systems, IQ imbalance compensation, massive MIMO, multi-user communication, transmitter IQ imbalance.

I. INTRODUCTION

The evolution of multiple-input multiple-output (MIMO) systems and their extension to large-scale MIMO or massive MIMO systems has gained immense popularity and will play a vital role in future wireless networks because of their capability to cater to the high throughput demand in multi-user (MU) communication, which can be achieved by using beamforming and spatial multiplexing supported by a large number of antennas at the base station (BS) [1]–[6]. The use of a large number of antennas results in several advantages over lower-dimensional MIMO systems, e.g., mutual orthogonality between the channel vectors of different users, mitigation of uncorrelated noise and intracell interference, and reduction in the required per user equipment (UE) transmit power [4]–[6]. Some of the recent works which studied different aspects of massive MIMO systems are [7]–[9]. Traditional MIMO systems have a separate radio-frequency (RF) chain for each antenna-element due to which these systems are also known as *fully-digital* (FD) MIMO systems. Therefore, FD massive MIMO systems can exploit all the spatial degrees-of-freedom (DoF) offered by the propagation channel, but their total cost and energy consumption will scale linearly with the number of antenna elements. However, massive MIMO systems serve only few UEs in each time-frequency resource due to which all the spatial DoF of the propagation channel are not exploited. This makes FD massive MIMO systems less attractive and unsuitable for large-scale deployment and hence low cost and less power hungry implementations are required.

Analog-beamforming systems (ABFSs) and hybrid-beamforming systems (HBFSs) are two economical and

The associate editor coordinating the review of this manuscript and approving it for publication was Irfan Ahmed.

energy-efficient MIMO architectures which can be used as alternatives to FD massive MIMO systems. In an ABFS, a single RF chain is connected to a large number of antennas through a phase-shifter network (PSN) to support single-stream transmission [10], while in an HBFS, a small number of RF chains are connected to a large antenna array through an analog precoder/combiner to enable multi-stream transmission [11], [12]. The number of RF chains in an HBFS is significantly smaller than the number of antennas and scales linearly with the number of UEs, thereby saving energy and system cost when compared to FD massive MIMO systems [11], [12]. Hence, an HBFS provides a trade-off between performance and cost, where performance can be improved by increasing the number of RF chains, while the cost can be decreased by reducing the number of RF chains.

The study of HBFSs has gained significant attention in the past few years and various architectures for HBFSs have been proposed to further improve the trade-off between complexity and performance. For example, a fully-connected architecture provides better design flexibility but at the cost of increased complexity since each RF chain is connected to each antenna-element through a PSN, a partially-connected architecture sacrifices some performance to reduce the complexity by connecting each RF chain to only a fixed subset of antenna-elements through a PSN, and a dynamically-connected architecture provides further trade-off between the performance and cost of fully-connected and partially-connected architectures by connecting each RF chain to a dynamically selected subset of antenna-elements through a PSN and a switching network [11], [12]. In the state-of-the-art, various algorithms for designing the hybrid precoder/combiner for different architectures of HBFSs operating in both rich and sparse channels have been proposed; these are based on either joint-design approach or two-stage approach [13]–[19] (for a more detailed review, please see the survey papers [11], [12]). The works [13]–[15] use a joint-design approach, whereas [16]–[19] use a two-stage approach to design the hybrid precoder/combiner. The downlink (DL) spectral efficiency (SE) and energy-efficiency (EE) of a PSN based massive MIMO HBFS with zero-forcing (ZF) precoding was investigated in [20], while different HBFS designs and their analysis with PSN and switches were presented in [21] and [22]. In [23], a minimum mean-square error (MMSE) based analog beamformer for a given analog to digital converter (ADC) resolution was derived and an online channel estimation technique was also proposed, while two hybrid beamforming techniques were proposed in [24] to reduce the cost and power consumption of a partially-connected architecture based massive MU-MIMO HBFS. For high-speed railway communication using HBFS, [25] proposed an angle domain channel tracking and hybrid beamforming scheme, which utilizes Kalman filtering and non-orthogonal beams, respectively. For practical channel estimation problems, [26] studied the trade-off between throughput and training duration in HBFSs along with MMSE channel estimation, whereas [27] and [28] provides channel estimation for rich scattering environments.

Most of the existing works on HBFSs assume the use of perfect transceivers which is not true in practical scenarios [29]. The use of low cost devices/components to reduce the transceiver cost gives rise to different types of hardware impairments [30]. In-phase (I) and quadrature-phase (Q) imbalance or IQ imbalance (IQI) is a hardware impairment which is found in direct-conversion transceivers. IQI refers to the amplitude and/or phase mismatch between the I and Q branches of an RF chain and is caused by the relative differences between the components used in both the branches. IQI is generally modeled as amplitude and/or phase errors introduced by the local oscillator (LO) in the RF chain [30].

The performance of MIMO and massive MIMO systems in the presence of hardware impairments (specially IQI) has been widely studied and a rich body of literature is available (please see [31]–[39] and references there-in). In contrast, the performance of HBFSs with hardware impairments is not well explored. The recent works which studied the performance of HBFSs in the presence of impairments other than IQI are [40]–[44], whereas the only relevant works considering HBFS with IQI are [45]–[47]. More specifically, in the context of FD-MIMO systems, the impact of receiver IQI on the performance of MIMO systems with a single RF chain was studied in [31] and a compensation algorithm was also proposed, while [32] extended the work of [31] to FD massive MU-MIMO systems and derived expressions for the sum SE and power scaling laws. Widely linear solutions for massive MIMO systems with IQI were proposed in [33] and [34], whereas massive MIMO systems with IQI and low resolution ADCs were investigated in [35]. The performance of the maximal ratio combining and ZF receivers in uplink (UL) massive MIMO systems with receiver IQI was studied in [36], while the performance limits of massive MIMO systems in the presence of both transmitter and receiver IQI were studied in [37]. The authors of [38] proposed a linear MMSE receiver for UL massive MIMO systems with random IQI, whereas [39] proposed a regularized ZF precoder for DL massive MIMO systems with IQI. However, none of the above works are directly applicable to HBFSs. Among the recent works which consider HBFSs with impairments other than IQI, [40] and [41] studied the performance of HBFS when non-linear effects of power amplifiers are considered, [42] studied the effects of residual transceiver hardware impairments in a point-to-point HBFS, [43] proposed a Householder based analog combiner to increase the sum-rate of a UL massive MU-MIMO HBFS for an ill-conditioned MIMO channel, and [44] studied the performance of a massive MU-MIMO HBFS with reciprocity calibration imperfections. However, IQI was not considered in [40]–[44]. Among the relevant works on HBFS with IQI, [45] studied the performance of mm-wave MU-MIMO HBFS with IQI by assuming perfect channel state information (CSI), but no IQI compensation algorithm was proposed. In [46], a single-user point-to-point mm-wave HBFS with only receiver IQI was considered and an

IQI compensation algorithm to mitigate the effects of receiver IQI was also proposed. However, the issue of transmitter IQI was not considered in [46] because of which the receiver IQI compensation algorithm proposed in [46] is unable to mitigate the effects of transmitter IQI. In [47], a single-user point-to-point mm-wave HBFS with only transmitter IQI was considered and an algorithm for the estimation and symbol level pre-compensation of transmitter IQI at the transmitter itself was proposed. The pre-compensation method proposed in [47] assumes the availability of instantaneous CSI at both the transmitter and the receiver, and hence is not applicable for the scenario where the transmitters are unaware of their instantaneous CSI.

A. CONTRIBUTIONS

From the above discussion, it is clear that the receiver IQI compensation algorithm proposed in [46] is unable to mitigate the effects of transmitter IQI. Also, for a typical UL massive MU-MIMO system where the estimate of instantaneous CSI is only available at the BS receiver (and not at the transmitting UEs) [48], it is not possible to apply the symbol level transmitter IQI pre-compensation algorithm of [47] at the transmitting UEs (since the transmitter IQI parameters are not available at the UEs for this scenario). An alternative solution to the above problem of mitigating the effects of transmitter IQI in a MU scenario is to compensate the effects of the UE's transmitter IQI at the BS receiver. This alternative solution is preferable over the pre-compensation algorithm of [47] because of the following two reasons: (1) As the BS is always aware of the estimate of the instantaneous CSI to implement the precoder/combiner [48], the suggested alternative solution is always applicable to compensate the transmitter IQI at the BS irrespective of whether the UEs are aware/unaware of their respective channels and IQI coefficients, (2) It reduces the real-time signal processing load at the UE side by shifting the implementation of the transmitter IQI compensation algorithm from the UE side to the BS side. It is worth mentioning that both [46] and [47] did not consider the MU scenario in the analysis and are limited to single-user point-to-point HBFSs operating in an mm-wave channel with the constraint that the number of RF chains at the transmitter and the receiver must be equal to the number of transmitted data-streams.

To the best of our knowledge, there is *no existing work* which proposes a transmitter IQI compensation algorithm for a UL massive MU-MIMO HBFS that is implemented at the BS receiver. Therefore, in this article, we consider a practical UL massive MU-MIMO HBFS having IQI primarily at the UEs[1] for which we propose a *novel* transmitter IQI compensation algorithm implemented at the BS receiver. The main contributions of this article are as follows:

1) We first show that when perfect CSI is available, uncompensated transmitter IQI causes a finite ceiling of the UL achievable sum-rate at high signal-to-noise ratio (SNR), which only depends upon the transmitter IQI matrices and is independent of the propagation channel and the choice of the hybrid combining matrices. This justifies the need for developing a transmitter IQI compensation algorithm for a UL massive MU-MIMO HBFS.
2) Next, we propose a *novel* ZF based transmitter IQI compensation algorithm implemented at the BS receiver, which effectively mitigates the undesired effects of transmitter IQI and is applicable for any channel model and any choice of the number of RF chains.
3) The sum-rate performance analysis of the proposed transmitter IQI compensation algorithm is presented and closed-form expression of the UL achievable sum-rate is derived for the large antenna regime (i.e., large number of BS antennas) and for the case where the channel is modeled by uncorrelated Rayleigh fading.
4) Finally, numerical results are presented for three different channel models which confirm that the proposed transmitter IQI compensation algorithm, implemented at the BS receiver, effectively mitigates the undesired effects of transmitter IQI in a UL massive MU-MIMO HBFS operating in different channel environments.

B. ORGANIZATION

This paper is organized as follows. The system model for the UL massive MU-MIMO HBFS with transmitter IQI is presented in Section II. The proposed transmitter IQI compensation algorithm and the performance analysis of the UL massive MU-MIMO HBFS with and without transmitter IQI compensation are presented in Section III. Numerical results are shown in Section IV, which demonstrate the effectiveness of the proposed transmitter IQI compensation algorithm. Finally, Section V gives the conclusion of the paper.

C. NOTATION

Here $|a|$ and $\angle a$ denote the absolute value and angle of scalar a, $[\mathbf{A}]_{m,n}$ denotes the element corresponding to the $(m,n)^{th}$ entry of the matrix $\mathbf{A}$, and $\mathbf{A}_{1:K}$ is a sub-matrix of $\mathbf{A}$ which consists of the first K columns of $\mathbf{A}$. $\mathbf{0}_{M\times N}$ and $\mathbf{1}_{M\times N}$ are, respectively, the $M \times N$ matrices of zeroes and ones, $\mathbf{I}_K$ is the $K \times K$ identity matrix, diag($\mathbf{a}$) is a diagonal matrix with the elements of vector $\mathbf{a}$ as its diagonal entries, and det$(\cdot)$ denotes the determinant of a square matrix. $\mathbb{E}[\cdot]$ and $Tr(\cdot)$ denote the expectation and trace operators, $j \triangleq \sqrt{-1}$, $\otimes$ denotes the Kronecker product, and the superscripts $(\cdot)^*$, $(\cdot)^T$, $(\cdot)^H$, $(\cdot)^{-1}$, $(\cdot)^{-*}$, and $(\cdot)^{-H}$ denote the conjugate, transpose, conjugate-transpose, inverse, conjugate-inverse, and conjugate-transpose-inverse operations, respectively. $\mathbb{R}$ and $\mathbb{C}$ denote the sets of real and complex numbers, respectively.

[1] In practical systems, cheaper and affordable UE design is realized by utilizing cheaper components having hardware imperfections which result in IQI at the UE, whereas a BS using precision components and devices is less prone to such imperfections.

For any $a, b \in \mathbb{R}$ and $b > a$, $Unif[a, b]$ denotes the uniform distribution between a and b.

II. SYSTEM MODEL

We consider the UL communication of a single-cell massive MU-MIMO HBFS where the BS is equipped with N antennas and N_{RF} ($N_{RF} \leq N$) RF chains to receive the symbols transmitted by K ($K \leq N_{RF}$) single-antenna UEs.[2] We assume that IQI exists at the transmit RF chain of each UE, whereas almost negligible or no IQI exists at the receive RF chains of the BS. Let x_k denote the desired baseband information symbol to be transmitted by the k^{th} UE where $k \in \{1, 2, \ldots, K\}$ and the symbols $\{x_k\}_{k=1}^{K}$ are independent and identically distributed (i.i.d.) zero-mean circularly-symmetric complex Gaussian (ZMCSCG) random variables having unit variance, i.e., $\mathbf{x} \triangleq [x_1, x_2, \ldots, x_K]^T \sim \mathcal{CN}(\mathbf{0}_{K\times 1}, \mathbf{I}_K)$. However, due to transmitter IQI, the desired symbols $\{x_k\}_{k=1}^{K}$ are not perfectly up-converted to the passband signal. Therefore, the baseband equivalent of the signal up-converted by the transmit RF chain of the k^{th} UE is given by [30]

$$\widetilde{x}_k = G_{1,k}x_k + G_{2,k}^{*}x_k^{*}, \tag{1}$$

where $G_{1,k}, G_{2,k} \in \mathbb{C}$ model the transmitter IQI at the k^{th} UE and are defined as [30]

$$G_{1,k} \triangleq \frac{1 + g_{T,k}e^{j\phi_{T,k}}}{2} \quad \text{and} \quad G_{2,k} \triangleq \frac{1 - g_{T,k}e^{-j\phi_{T,k}}}{2}, \tag{2}$$

where $g_{T,k} \in \mathbb{R}^{+}$ and $\phi_{T,k} \in \mathbb{R}$, respectively, model the amplitude and phase mismatch at the transmit RF chain of the k^{th} UE.[3] Also, $G_{1,k}$ and $G_{2,k}$ satisfy $G_{1,k} + G_{2,k}^{*} = 1$. In the absence of transmitter IQI, $g_{T,k} = 1$ and $\phi_{T,k} = 0$ which implies $G_{1,k} = 1$ and $G_{2,k} = 0$, and hence (1) reduces to $\widetilde{x}_k = x_k$ which represents perfect up-conversion at the k^{th} UE. Therefore, from (1) and (2), the $K \times 1$ symbol vector which consists of baseband equivalent of the symbols up-converted by K UEs can be written as

$$\widetilde{\mathbf{x}} = \mathbf{G}_1\mathbf{x} + \mathbf{G}_2^{*}\mathbf{x}^{*}, \tag{3}$$

where $\widetilde{\mathbf{x}} \triangleq [\widetilde{x}_1, \widetilde{x}_2, \ldots, \widetilde{x}_K]^T$, $\mathbf{G}_1 \triangleq \text{diag}(G_{1,1}, G_{1,2}, \ldots, G_{1,K})$, and $\mathbf{G}_2 \triangleq \text{diag}(G_{2,1}, G_{2,2}, \ldots, G_{2,K})$. From (2) we note that the IQI matrices $\mathbf{G}_1$ and $\mathbf{G}_2$ satisfy $\mathbf{G}_1 + \mathbf{G}_2^{*} = \mathbf{I}_K$. The up-converted signal at each UE is passed through the power amplifier and then transmitted through its antenna, which, after propagating through the wireless channel, is received at the antenna array of the BS. Hence, the baseband equivalent of the $N \times 1$ signal vector received at the antenna array of the BS is given by

$$\mathbf{y} = \sqrt{\rho_u}\mathbf{H}\widetilde{\mathbf{x}} + \mathbf{n}, \tag{4}$$

where ρ_u is the average power transmitted by each UE, $\mathbf{H} \in \mathbb{C}^{N\times K}$ is the propagation channel matrix between the UEs and BS antennas where each entry of $\mathbf{H}$ is a zero-mean random variable ($\mathbb{E}\left[[\mathbf{H}]_{n,k}\right] = 0$),[4] and $\mathbf{n} \in \mathbb{C}^{N\times 1}$ is the additive white Gaussian noise (AWGN) vector at the antenna array of the BS whose components are i.i.d. ZMCSCG random variables with variance σ_n^2, i.e., $\mathbf{n} \sim \mathcal{CN}(\mathbf{0}_{N\times 1}, \sigma_n^2\mathbf{I}_N)$.

Next, the received signal vector at the BS is passed through a hybrid combiner (analog combiner $\mathbf{W}_{RF}$ and digital combiner $\mathbf{W}_{BB}$) which converts the received N-dimensional symbol vector to an N_{RF}-dimensional vector and then to a K-dimensional vector to produce an estimate of $\mathbf{x}$. We assume that the analog combiner $\mathbf{W}_{RF} \in \mathbb{C}^{N\times N_{RF}}$ is implemented by using a fully-connected PSN [16], [17]. Since the phase-shifters cannot change the magnitude of the incoming signal, there is a constant magnitude constraint on the entries of $\mathbf{W}_{RF}$, i.e., $[\mathbf{W}_{RF}]_{n,p} = \frac{1}{\sqrt{N}}e^{j\phi_{n,p}}$, where $\phi_{n,p} \in \mathbb{R}$ is the phase-shift provided by the phase-shifter corresponding to the $(n, p)^{th}$ entry of $\mathbf{W}_{RF}$, $n \in \{1, 2, \ldots, N\}$, $p \in \{1, 2, \ldots, N_{RF}\}$, and the factor $1/\sqrt{N}$ ensures that the $\mathcal{L}2$-norm of each column of $\mathbf{W}_{RF}$ is unity. The signal received at the output of the analog combiner is down-converted by the RF chains of the BS after which the BS applies the digital combiner $\mathbf{W}_{BB} \in \mathbb{C}^{N_{RF}\times K}$ to produce the estimate of $\mathbf{x}$. Therefore, using (3) and (4), the $K \times 1$ symbol vector obtained at the output of the digital combiner is given by

$$\begin{aligned}\mathbf{y}_{BB} &\triangleq \mathbf{W}_{BB}^{H}\mathbf{W}_{RF}^{H}\mathbf{y} \\ &= \sqrt{\rho_u}\mathbf{W}_{BB}^{H}\mathbf{W}_{RF}^{H}\mathbf{H}\widetilde{\mathbf{x}} + \mathbf{W}_{BB}^{H}\mathbf{W}_{RF}^{H}\mathbf{n} \\ &= \sqrt{\rho_u}\mathbf{H}_{DS}\mathbf{x} + \sqrt{\rho_u}\mathbf{H}_{IQ}\mathbf{x}^{*} + \mathbf{n}_{BB},\end{aligned} \tag{5}$$

where $\mathbf{H}_{DS} \triangleq \mathbf{W}_{BB}^{H}\mathbf{W}_{RF}^{H}\mathbf{H}\mathbf{G}_1 \in \mathbb{C}^{K\times K}$ is the effective primary channel corresponding to the desired signal, $\mathbf{H}_{IQ} \triangleq \mathbf{W}_{BB}^{H}\mathbf{W}_{RF}^{H}\mathbf{H}\mathbf{G}_2^{*} \in \mathbb{C}^{K\times K}$ is the effective IQI interference channel created by the transmitter IQI, and $\mathbf{n}_{BB} \triangleq \mathbf{W}_{BB}^{H}\mathbf{W}_{RF}^{H}\mathbf{n} \in \mathbb{C}^{K\times 1}$ is the receiver noise after digital combining.

III. PERFORMANCE ANALYSIS

In this section, we first show that when the SNR approaches infinity, the uncompensated transmitter IQI causes a finite ceiling of the UL achievable sum-rate which only depends upon the transmitter IQI parameters and is independent of the propagation channel and the choice of the hybrid combining matrices. This justifies the need for developing a transmitter IQI compensation algorithm for a UL massive MU-MIMO HBFS. Therefore, we propose a novel ZF based transmitter IQI compensation algorithm to be implemented at the BS, which effectively eliminates the undesired effects of transmitter IQI, and is applicable for any channel model and any choice of $\mathbf{W}_{RF}$, $\mathbf{W}_{BB}$, N, N_{RF}, and K. Finally, for the uncorrelated Rayleigh fading channel and large antenna

[2]The proposed transmitter IQI compensation algorithm in this work can be extended to the case where each UE is also equipped with multiple antennas, which is left for future work.

[3]In the state-of-the-art, two different IQI modeling methods are known: (i) Symmetrical method, (ii) Asymmetrical method. It is well known that these two IQI modeling methods are equivalent [30]. Therefore, we use the asymmetrical method to model the transmitter IQI.

[4]The zero-mean channel coefficients are assumed only to simplify the performance analysis. However, the transmitter IQI compensation algorithm proposed in Subsection III-B is also valid for channels having non-zero mean.

regime ($N \to \infty$), we derive an approximate closed-form expression of the UL sum-rate achieved by the effective massive MU-MIMO HBFS with the proposed transmitter IQI compensation.

A. PERFORMANCE ANALYSIS WITH NO TRANSMITTER IQI COMPENSATION

When the BS receiver is unaware of the presence of transmitter IQI at the UEs, it does not apply any transmitter IQI compensation algorithm, and hence we can rewrite (5) as

$$\mathbf{y}_{BB} = \sqrt{\rho_u}\mathbf{H}_{DS}\mathbf{x} + \mathbf{n}_e, \tag{6}$$

where $\sqrt{\rho_u}\mathbf{H}_{DS}\mathbf{x}$ is the desired signal term, and $\mathbf{n}_e \triangleq \sqrt{\rho_u}\mathbf{H}_{IQ}\mathbf{x}^* + \mathbf{n}_{BB}$ is the effective interference plus noise vector which consists of the IQI interference term ($\sqrt{\rho_u}\mathbf{H}_{IQ}\mathbf{x}^*$) and the receiver noise after digital combining ($\mathbf{n}_{BB}$). It is important to note that $\mathbf{n}_e$ and $\mathbf{x}$ are statistically uncorrelated random vectors, i.e,

$$\begin{aligned}\mathbb{E}\left[\mathbf{n}_e\mathbf{x}^H\right] &= \mathbb{E}\left[(\sqrt{\rho_u}\,\mathbf{H}_{IQ}\mathbf{x}^* + \mathbf{n}_{BB})\mathbf{x}^H\right] \\ &= \sqrt{\rho_u}\,\mathbf{H}_{IQ}\,\mathbb{E}\left[(\mathbf{x}\mathbf{x}^T)^*\right] + \mathbf{W}_{BB}^H\mathbf{W}_{RF}^H\,\mathbb{E}\left[\mathbf{n}\mathbf{x}^H\right] \\ &= \mathbf{0}_{K\times K},\end{aligned} \tag{7}$$

where we have used the definition of $\mathbf{n}_{BB}$, circular-symmetry property of the vector $\mathbf{x}$ $\left(\mathbb{E}\left[(\mathbf{x}\mathbf{x}^T)\right] = \mathbf{0}_{K\times K}\right)$, and statistical independence of the zero-mean vectors $\mathbf{n}$ and $\mathbf{x}$ $\left(\mathbb{E}\left[\mathbf{n}\mathbf{x}^H\right] = \mathbb{E}\left[\mathbf{n}\right]\mathbb{E}\left[\mathbf{x}^H\right] = \mathbf{0}_{N\times K}\right)$. Hence, for a given $(\mathbf{H}, \mathbf{G}_1, \mathbf{G}_2, \mathbf{W}_{RF}, \mathbf{W}_{BB})$, the UL achievable sum-rate of the transmitter IQI uncompensated UL massive MU-MIMO HBFS is given by [49]

$$\begin{aligned}R_{sum}^{NC} &= \log_2\det\left(\mathbf{I}_K + \rho_u\,\mathbf{K}_{n_e}^{-1}\mathbf{H}_{DS}\mathbf{H}_{DS}^H\right) \\ &= \log_2\det\Big(\mathbf{I}_K + \rho_u\,\mathbf{K}_{n_e}^{-1}\mathbf{W}_{BB}^H\mathbf{W}_{RF}^H\mathbf{H}\mathbf{G}_1 \\ &\quad\times\mathbf{G}_1^H\mathbf{H}^H\mathbf{W}_{RF}\mathbf{W}_{BB}\Big),\end{aligned} \tag{8}$$

where the superscript '*NC*' stands for *no compensation*, and $\mathbf{K}_{n_e}$ is the covariance matrix of $\mathbf{n}_e$ and is given by

$$\begin{aligned}\mathbf{K}_{n_e} &= \rho_u\,\mathbf{H}_{IQ}\mathbf{H}_{IQ}^H + \sigma_n^2\,\mathbf{W}_{BB}^H\mathbf{W}_{RF}^H\mathbf{W}_{RF}\mathbf{W}_{BB} \\ &= \rho_u\,\mathbf{W}_{BB}^H\mathbf{W}_{RF}^H\mathbf{H}\mathbf{G}_2^*\mathbf{G}_2^T\mathbf{H}^H\mathbf{W}_{RF}\mathbf{W}_{BB} \\ &\quad+\sigma_n^2\,\mathbf{W}_{BB}^H\mathbf{W}_{RF}^H\mathbf{W}_{RF}\mathbf{W}_{BB}.\end{aligned} \tag{9}$$

The expression in (8) is a general result which can be used to find the UL achievable sum-rate of the transmitter IQI uncompensated UL massive MU-MIMO HBFS for any choice of hybrid combining matrices $\mathbf{W}_{RF}$ and $\mathbf{W}_{BB}$. In the following lemma, we discuss the behavior of R_{sum}^{NC} in the high-SNR regime.

Lemma 1: In the high-SNR regime, i.e., when ρ_u/σ_n^2 goes to infinity, the UL achievable sum-rate in (8) *converges to $R_{sum,ceil}^{NC}$, where $R_{sum,ceil}^{NC} \triangleq \lim_{\rho_u/\sigma_n^2\to\infty} R_{sum}^{NC}$ and is given by*

$$\lim_{\rho_u/\sigma_n^2\to\infty} R_{sum}^{NC} = \log_2\det\left(\mathbf{I}_K + (\mathbf{G}_2\mathbf{G}_2^H)^{-1}\mathbf{G}_1\mathbf{G}_1^H\right). \tag{10}$$

Proof: Please see Appendix A. ■

Lemma 1 states that in the high-SNR regime, the UL achievable sum-rate of the transmitter IQI uncompensated UL massive MU-MIMO HBFS does not increase with increasing SNR and is limited by the asymptotic sum-rate expression given by (10) which only depends upon the transmitter IQI matrices $\mathbf{G}_1$ and $\mathbf{G}_2$. It is due to the fact that when the SNR increases, the IQI interference term ($\sqrt{\rho_u}\mathbf{H}_{IQ}\mathbf{x}^*$) in (6) also starts increasing and becomes the dominating term of the effective interference plus noise vector $\mathbf{n}_e$. Hence, the covariance matrix in (9) can be approximated as $\mathbf{K}_{n_e} \approx \rho_u\,\mathbf{H}_{IQ}\mathbf{H}_{IQ}^H$ and after substituting it in (8), the UL achievable sum-rate expression becomes independent of the SNR which results in a finite ceiling of the sum-rate. However, when there is no transmitter IQI ($\mathbf{G}_1 = \mathbf{I}_K$, $\mathbf{G}_2 = \mathbf{0}_{K\times K}$), $\mathbf{H}_{IQ}$ in (5) becomes $\mathbf{0}_{K\times K}$ due to which (9) reduces to $\sigma_n^2\,\mathbf{W}_{BB}^H\mathbf{W}_{RF}^H\mathbf{W}_{RF}\mathbf{W}_{BB}$ and becomes independent of the transmit power. Hence, if there is no transmitter IQI, R_{sum}^{NC} in (8) will not ceil at high SNR. Therefore, to achieve a high sum-rate in the presence of transmitter IQI, compensation of transmitter IQI is required in UL massive MU-MIMO HBFS.

B. ZERO-FORCING BASED TRANSMITTER IQI COMPENSATION ALGORITHM

To mitigate the undesired effects of IQI caused by UE transmitters, we propose a novel ZF based transmitter IQI compensation algorithm for the UL massive MU-MIMO HBFS which is implemented at the BS receiver and is applicable for any choice of $\mathbf{H}$, $\mathbf{W}_{RF}$, and $\mathbf{W}_{BB}$. We assume that the BS has perfect prior knowledge of the channel matrix $\mathbf{H}$ and the UE's transmitter IQI parameters ($\{G_{1,k}\}_{k=1}^K$, $\{G_{2,k}\}_{k=1}^K$), which are required to design the proposed transmitter IQI compensation algorithm.[5]

After vertically concatenating the received symbol vector $\mathbf{y}_{BB}$ given in (5) and its complex-conjugate, the composite system model is given by

$$\mathbf{y}_C = \sqrt{\rho_u}\,\mathbf{H}_C\mathbf{x}_C + \mathbf{n}_C, \tag{11}$$

where $\mathbf{y}_C \triangleq \begin{bmatrix}\mathbf{y}_{BB}\\ \mathbf{y}_{BB}^*\end{bmatrix} \in \mathbb{C}^{2K\times 1}$, $\mathbf{H}_C \triangleq \begin{bmatrix}\mathbf{H}_{DS} & \mathbf{H}_{IQ}\\ \mathbf{H}_{IQ}^* & \mathbf{H}_{DS}^*\end{bmatrix} \in \mathbb{C}^{2K\times 2K}$, $\mathbf{x}_C \triangleq \begin{bmatrix}\mathbf{x}\\ \mathbf{x}^*\end{bmatrix} \in \mathbb{C}^{2K\times 1}$, and $\mathbf{n}_C \triangleq \begin{bmatrix}\mathbf{n}_{BB}\\ \mathbf{n}_{BB}^*\end{bmatrix} \in \mathbb{C}^{2K\times 1}$. Using the definitions of $\mathbf{H}_{DS}$ and $\mathbf{H}_{IQ}$, we can factorize $\mathbf{H}_C$ as

$$\begin{aligned}\mathbf{H}_C &= \begin{bmatrix}\mathbf{W}_{BB}^H\mathbf{W}_{RF}^H\mathbf{H}\mathbf{G}_1 & \mathbf{W}_{BB}^H\mathbf{W}_{RF}^H\mathbf{H}\mathbf{G}_2^*\\ (\mathbf{W}_{BB}^H\mathbf{W}_{RF}^H\mathbf{H}\mathbf{G}_2^*)^* & (\mathbf{W}_{BB}^H\mathbf{W}_{RF}^H\mathbf{H}\mathbf{G}_1)^*\end{bmatrix} \\ &= \begin{bmatrix}\mathbf{W}_{BB}^H\mathbf{W}_{RF}^H\mathbf{H} & \mathbf{0}_{K\times K}\\ \mathbf{0}_{K\times K} & (\mathbf{W}_{BB}^H\mathbf{W}_{RF}^H\mathbf{H})^*\end{bmatrix}\begin{bmatrix}\mathbf{G}_1 & \mathbf{G}_2^*\\ \mathbf{G}_2 & \mathbf{G}_1^*\end{bmatrix},\end{aligned} \tag{12}$$

where it is easy to verify that each factor matrix of $\mathbf{H}_C$ in (12) is invertible. The invertibility of the first factor matrix can

[5] In practical systems, perfect and prior knowledge of $\mathbf{H}$, $\{G_{1,k}\}_{k=1}^K$, and $\{G_{2,k}\}_{k=1}^K$ is never available. Instead, these parameters can be estimated by using training based methods or blind estimation techniques. The performance analysis of the proposed transmitter IQI compensation algorithm with estimated CSI is left for future work and is beyond the scope of this paper.

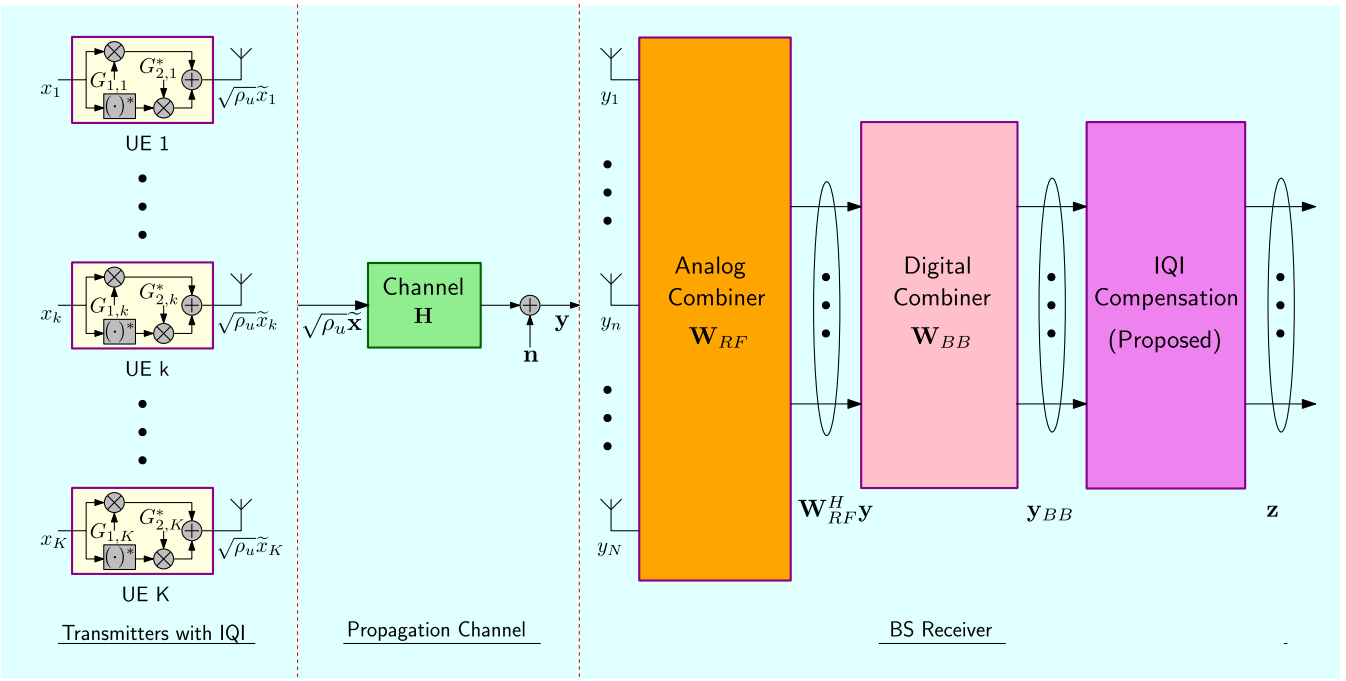

FIGURE 1. Block diagram of a UL massive MU-MIMO HBFS with transmitter IQI and the proposed transmitter IQI compensation.

be verified by exploiting its block-diagonal structure and the full rank property of $\mathbf{W}_{BB}^H\mathbf{W}_{RF}^H\mathbf{H}$ (please see the discussion in Appendix A), whereas the second factor matrix can be shown to be invertible by using the block matrix inversion lemma [50] and the full-rank property of $\mathbf{G}_1$ ($\mathbf{G}_1$ is a diagonal matrix with non-zero diagonal entries and hence is always full rank). Therefore, the matrix $\mathbf{H}_C$ is also invertible and the inverse is given by

$$\mathbf{H}_C^{-1} = \begin{bmatrix} \mathbf{\Phi}_1 & \mathbf{\Phi}_2 \\ \mathbf{\Phi}_2^* & \mathbf{\Phi}_1^* \end{bmatrix} \begin{bmatrix} (\mathbf{W}_{BB}^H\mathbf{W}_{RF}^H\mathbf{H})^{-1} & \mathbf{0}_{K\times K} \\ \mathbf{0}_{K\times K} & (\mathbf{W}_{BB}^H\mathbf{W}_{RF}^H\mathbf{H})^{-*} \end{bmatrix}, \quad (13)$$

where we have used the property $(\mathbf{AB})^{-1} = \mathbf{B}^{-1}\mathbf{A}^{-1}$, and $\begin{bmatrix} \mathbf{\Phi}_1 & \mathbf{\Phi}_2 \\ \mathbf{\Phi}_2^* & \mathbf{\Phi}_1^* \end{bmatrix} \triangleq \begin{bmatrix} \mathbf{G}_1 & \mathbf{G}_2^* \\ \mathbf{G}_2 & \mathbf{G}_1^* \end{bmatrix}^{-1}$, where $\mathbf{\Phi}_1$ and $\mathbf{\Phi}_2$ can be obtained by using the block matrix inversion lemma [50] and are given by $\mathbf{\Phi}_1 = \left(\mathbf{G}_1 - \mathbf{G}_2^*\mathbf{G}_1^{-*}\mathbf{G}_2\right)^{-1}$ and $\mathbf{\Phi}_2 = -\mathbf{G}_1^{-1}\mathbf{G}_2^*\mathbf{\Phi}_1^*$. We note that $\mathbf{\Phi}_1$ and $\mathbf{\Phi}_2$ are also diagonal matrices (since $\mathbf{G}_1$ and $\mathbf{G}_2$ are diagonal matrices) and can be easily computed.

Hence, the transmitter IQI compensation for the UL massive MU-MIMO HBFS considered in this paper can be performed by pre-multiplying $\mathbf{y}_C$ in (11) by $\mathbf{H}_C^{-1}$ which gives

$$\mathbf{H}_C^{-1}\mathbf{y}_C = \sqrt{\rho_u}\,\mathbf{x}_C + \mathbf{H}_C^{-1}\mathbf{n}_C, \quad (14)$$

where the proposed transmitter IQI compensation technique makes the information symbol vector free from transmitter IQI and the term $\mathbf{H}_C^{-1}\mathbf{n}_C$ can be further simplified as

$$\begin{aligned}\mathbf{H}_C^{-1}\mathbf{n}_C &= \mathbf{H}_C^{-1}\begin{bmatrix} \mathbf{n}_{BB} \\ \mathbf{n}_{BB}^* \end{bmatrix} = \mathbf{H}_C^{-1}\begin{bmatrix} \mathbf{W}_{BB}^H\mathbf{W}_{RF}^H\mathbf{n} \\ (\mathbf{W}_{BB}^H\mathbf{W}_{RF}^H\mathbf{n})^* \end{bmatrix} \\ &= \begin{bmatrix} \mathbf{\Phi}_1 & \mathbf{\Phi}_2 \\ \mathbf{\Phi}_2^* & \mathbf{\Phi}_1^* \end{bmatrix}\begin{bmatrix} (\mathbf{W}_{BB}^H\mathbf{W}_{RF}^H\mathbf{H})^{-1} & \mathbf{0}_{K\times K} \\ \mathbf{0}_{K\times K} & (\mathbf{W}_{BB}^H\mathbf{W}_{RF}^H\mathbf{H})^{-*} \end{bmatrix} \\ &\quad \times \begin{bmatrix} \mathbf{W}_{BB}^H\mathbf{W}_{RF}^H\mathbf{n} \\ (\mathbf{W}_{BB}^H\mathbf{W}_{RF}^H\mathbf{n})^* \end{bmatrix} \\ &= \begin{bmatrix} \mathbf{\Phi}_1 & \mathbf{\Phi}_2 \\ \mathbf{\Phi}_2^* & \mathbf{\Phi}_1^* \end{bmatrix}\begin{bmatrix} (\mathbf{W}_{BB}^H\mathbf{W}_{RF}^H\mathbf{H})^{-1}\mathbf{W}_{BB}^H\mathbf{W}_{RF}^H\mathbf{n} \\ \left((\mathbf{W}_{BB}^H\mathbf{W}_{RF}^H\mathbf{H})^{-1}\mathbf{W}_{BB}^H\mathbf{W}_{RF}^H\mathbf{n}\right)^* \end{bmatrix} \\ &= \begin{bmatrix} \mathbf{\Phi}_1\widehat{\mathbf{n}} + \mathbf{\Phi}_2\widehat{\mathbf{n}}^* \\ (\mathbf{\Phi}_1\widehat{\mathbf{n}} + \mathbf{\Phi}_2\widehat{\mathbf{n}}^*)^* \end{bmatrix}, \end{aligned} \quad (15)$$

where $\widehat{\mathbf{n}} \triangleq (\mathbf{W}_{BB}^H\mathbf{W}_{RF}^H\mathbf{H})^{-1}\mathbf{W}_{BB}^H\mathbf{W}_{RF}^H\mathbf{n}$ is a zero-mean random vector, and (15) is obtained by using the definitions of $\mathbf{n}_C$ and $\mathbf{n}_{BB}$, the factorization of $\mathbf{H}_C^{-1}$ from (13), and the identity $(\mathbf{AB})^* = \mathbf{A}^*\mathbf{B}^*$. From (15), it is clear that the effective noise $\mathbf{H}_C^{-1}\mathbf{n}_C$ does not depend on the transmit power ρ_u and hence the proposed transmitter IQI compensation algorithm solves the problem of ceiling of achievable sum-rate at high SNR. Finally, pre-multiplying (14) by $\begin{bmatrix} \mathbf{I}_K & \mathbf{0}_{K\times K} \end{bmatrix}$, we get,

$$\begin{aligned}\mathbf{z} &\triangleq \begin{bmatrix} \mathbf{I}_K & \mathbf{0}_{K\times K} \end{bmatrix}\mathbf{H}_C^{-1}\mathbf{y}_C \\ &\overset{(a)}{=} \begin{bmatrix} \mathbf{I}_K & \mathbf{0}_{K\times K} \end{bmatrix}\left(\sqrt{\rho_u}\begin{bmatrix} \mathbf{x} \\ \mathbf{x}^* \end{bmatrix} + \begin{bmatrix} \mathbf{\Phi}_1\widehat{\mathbf{n}} + \mathbf{\Phi}_2\widehat{\mathbf{n}}^* \\ (\mathbf{\Phi}_1\widehat{\mathbf{n}} + \mathbf{\Phi}_2\widehat{\mathbf{n}}^*)^* \end{bmatrix}\right) \\ &= \sqrt{\rho_u}\,\mathbf{x} + \mathbf{\Phi}_1\widehat{\mathbf{n}} + \mathbf{\Phi}_2\widehat{\mathbf{n}}^* \\ &\overset{(b)}{=} \sqrt{\rho_u}\,\mathbf{x} + \mathbf{\Phi}_1\widehat{\mathbf{n}} - \mathbf{G}_1^{-1}\mathbf{G}_2^*\mathbf{\Phi}_1^*\widehat{\mathbf{n}}^* \\ &= \sqrt{\rho_u}\,\mathbf{x} + \widetilde{\mathbf{n}}, \end{aligned} \quad (16)$$

where (a) is obtained by substituting the expression of $\mathbf{H}_C^{-1}\mathbf{n}_C$ from (15) in (14), (b) is obtained by using the definition of $\mathbf{\Phi}_2$, and $\widetilde{\mathbf{n}} \triangleq \left(\mathbf{\Phi}_1\widehat{\mathbf{n}} - \mathbf{G}_1^{-1}\mathbf{G}_2^*\mathbf{\Phi}_1^*\widehat{\mathbf{n}}^*\right)$ is a zero-mean random vector representing the effective noise after transmitter IQI compensation.

Next, we present the sum-rate performance analysis of the effective massive MU-MIMO HBFS obtained after applying the proposed transmitter IQI compensation algorithm.

C. PERFORMANCE ANALYSIS WITH TRANSMITTER IQI COMPENSATION

As $\mathbf{x}$ and $\mathbf{n}$ are statistically independent random vectors, from the definition of $\widetilde{\mathbf{n}}$ and $\widehat{\mathbf{n}}$, it follows that $\mathbf{x}$ and $\widetilde{\mathbf{n}}$ are also statistically independent and hence uncorrelated. Therefore, from (16) and for a given $(\mathbf{H}, \mathbf{G}_1, \mathbf{G}_2, \mathbf{W}_{RF}, \mathbf{W}_{BB})$, the UL achievable sum-rate of the proposed transmitter IQI compensated MU-MIMO HBFS is given by [49]

$$R_{sum}^{WC} = \log_2 \det\left(\mathbf{I}_K + \rho_u \mathbf{K}_{\widetilde{n}}^{-1}\right), \tag{17}$$

where the superscript '*WC*' stands for *with IQI-compensation* and $\mathbf{K}_{\widetilde{n}}$ is the covariance matrix of $\widetilde{\mathbf{n}}$ which is given by

$$\begin{aligned}\mathbf{K}_{\widetilde{n}} &= \mathbb{E}\left[\left(\mathbf{\Phi}_1\widehat{\mathbf{n}} - \mathbf{G}_1^{-1}\mathbf{G}_2^*\mathbf{\Phi}_1^*\widehat{\mathbf{n}}^*\right)\left(\mathbf{\Phi}_1\widehat{\mathbf{n}} - \mathbf{G}_1^{-1}\mathbf{G}_2^*\mathbf{\Phi}_1^*\widehat{\mathbf{n}}^*\right)^H\right] \\ &= \mathbf{\Phi}_1\mathbf{K}_{\widehat{n}}\mathbf{\Phi}_1^H + \mathbf{G}_1^{-1}\mathbf{G}_2^*\mathbf{\Phi}_1^*\mathbf{K}_{\widehat{n}^*}\mathbf{\Phi}_1^T\mathbf{G}_2^T\mathbf{G}_1^{-H}, \end{aligned} \tag{18}$$

where $\mathbf{K}_{\widehat{n}}$ and $\mathbf{K}_{\widehat{n}^*}$ are, respectively, the covariance matrices of $\widehat{\mathbf{n}}$ and $\widehat{\mathbf{n}}^*$, and are given by

$$\begin{aligned}\mathbf{K}_{\widehat{n}} &= \mathbb{E}\left[\left((\mathbf{W}_{BB}^H\mathbf{W}_{RF}^H\mathbf{H})^{-1}\mathbf{W}_{BB}^H\mathbf{W}_{RF}^H\mathbf{n}\right)\right. \\ &\quad \left.\times\left((\mathbf{W}_{BB}^H\mathbf{W}_{RF}^H\mathbf{H})^{-1}\mathbf{W}_{BB}^H\mathbf{W}_{RF}^H\mathbf{n}\right)^H\right] \\ &= \sigma_n^2(\mathbf{W}_{BB}^H\mathbf{W}_{RF}^H\mathbf{H})^{-1}\mathbf{W}_{BB}^H\mathbf{W}_{RF}^H \\ &\quad \times \mathbf{W}_{RF}\mathbf{W}_{BB}(\mathbf{W}_{BB}^H\mathbf{W}_{RF}^H\mathbf{H})^{-H}, \end{aligned} \tag{19}$$

$$\text{and} \quad \mathbf{K}_{\widehat{n}^*} = \mathbb{E}\left[(\widehat{\mathbf{n}}^*)(\widehat{\mathbf{n}}^*)^H\right] = \mathbf{K}_{\widehat{n}}^*. \tag{20}$$

The expression in (17) is a *general* result which can be used to find the UL achievable sum-rate of the effective massive MU-MIMO HBFS obtained after applying the proposed transmitter IQI compensation algorithm for any choice of $\mathbf{H}$, $\mathbf{W}_{RF}$, $\mathbf{W}_{BB}$, N, N_{RF}, and K. Next, we examine the sum-rate performance of (17) for three different channel models, namely, (i) uncorrelated Rayleigh fading channels, (ii) correlated Rayleigh fading channels, and (iii) sparse mm-wave channels. For the uncorrelated Rayleigh fading channels, we derive an approximate closed-form expression of R_{sum}^{WC} which provides useful insights regarding the dependence of R_{sum}^{WC} on IQI parameters, while, for correlated Rayleigh fading channels and sparse mm-wave channels, numerical simulations are provided which justify the effectiveness of the proposed transmitter IQI compensation algorithm.

As $K \leq N_{RF} \leq N$ and it is well known that the HBFSs with $N_{RF} = 2K$ are able to implement fully-digital combiners by properly designing $\mathbf{W}_{RF}$ and $\mathbf{W}_{BB}$, we consider the range $K \leq N_{RF} \leq 2K$ which is of practical interest and is widely studied in the state-of-the-art [16], [17]. It is worth mentioning that the hybrid combiners in this paper are designed by modifying the hybrid precoders of [17], which were originally designed for the DL scenario. As the hybrid precoders of [17] for $N_{RF} = K$, $N_{RF} = 2K$, and $K < N_{RF} < 2K$ scenarios are different and these cases were studied individually in [17], it is not possible to directly obtain a single closed-form expression of R_{sum}^{WC} when $K \leq N_{RF} \leq 2K$. Hence, we derive approximate closed-form expressions of R_{sum}^{WC} for $N_{RF} = K$ and $N_{RF} = 2K$ scenarios when uncorrelated Rayleigh fading is assumed; using these an approximate closed-form expression of R_{sum}^{WC} for the $K \leq N_{RF} \leq 2K$ scenario is derived.

1) PERFORMANCE ANALYSIS FOR $N_{RF} = K$ SCENARIO

In this section, we present the asymptotically ($N \to \infty$) optimal design of $\mathbf{W}_{RF}$ and $\mathbf{W}_{BB}$ for the $N_{RF} = K$ scenario; using this an approximate closed-form expression of R_{sum}^{WC} in the large antenna regime is derived for uncorrelated Rayleigh fading.

For the $N_{RF} = K$ scenario, $\mathbf{W}_{BB}$ and $\mathbf{W}_{RF}^H\mathbf{H}$ become square matrices of order K (as, $\mathbf{W}_{BB} \in \mathbb{C}^{N_{RF}\times K}$, $\mathbf{W}_{RF} \in \mathbb{C}^{N\times N_{RF}}$, and $\mathbf{H} \in \mathbb{C}^{N\times K}$) due to which the matrix $(\mathbf{W}_{BB}^H\mathbf{W}_{RF}^H\mathbf{H})^{-1}$ in (19) can be factorized as $(\mathbf{W}_{RF}^H\mathbf{H})^{-1}(\mathbf{W}_{BB}^H)^{-1}$ and hence, (19) simplifies to

$$\begin{aligned}\mathbf{K}_{\widehat{n}} &= \sigma_n^2(\mathbf{W}_{RF}^H\mathbf{H})^{-1}\mathbf{W}_{BB}^{-H}\mathbf{W}_{BB}^H\mathbf{W}_{RF}^H \\ &\quad \times \mathbf{W}_{RF}\mathbf{W}_{BB}\mathbf{W}_{BB}^{-1}(\mathbf{W}_{RF}^H\mathbf{H})^{-H} \\ &= \sigma_n^2(\mathbf{W}_{RF}^H\mathbf{H})^{-1}\mathbf{W}_{RF}^H\mathbf{W}_{RF}(\mathbf{W}_{RF}^H\mathbf{H})^{-H}, \end{aligned} \tag{21}$$

which shows that $\mathbf{K}_{\widehat{n}}$ becomes *independent* of $\mathbf{W}_{BB}$ for the $N_{RF} = K$ scenario. Hence, from (17), (18), (20), and (21), it can be concluded that for the $N_{RF} = K$ scenario, the UL achievable sum-rate R_{sum}^{WC} also becomes *independent* of $\mathbf{W}_{BB}$ because of which any full-rank $\mathbf{W}_{BB}$ can be chosen and we only have to find the optimal RF combiner $\mathbf{W}_{RF}$. Therefore, we choose $\mathbf{W}_{BB} = \mathbf{I}_K$, whereas the asymptotically optimal RF combiner for the $N_{RF} = K$ scenario is given in Lemma 2.

Lemma 2: For an IQI-free massive MU-MIMO HBFS with $N_{RF} = K$, the asymptotically optimal RF combiner in the large antenna limit is given by

$$[\mathbf{W}_{RF}^{opt}]_{n,k} = \frac{1}{\sqrt{N}} e^{j\angle U_{n,k}}, \tag{22}$$

where $e^{j\angle U_{n,k}} = U_{n,k}/|U_{n,k}|$, $U_{n,k} \triangleq [\mathbf{U}]_{n,k}$, $\mathbf{U} \in \mathbb{C}^{N\times N}$ is a unitary matrix consisting of left singular vectors of $\mathbf{H}$, $n \in \{1, 2, \ldots, N\}$, and $k \in \{1, 2, \ldots, K\}$.

Proof: Please see Appendix B. ∎

The reason behind choosing the RF combiner given in Lemma 2 is that firstly, it is the asymptotically optimal solution for the no IQI scenario, the choice of which enables a fair comparison between the performance of the transmitter IQI impaired massive MU-MIMO HBFS with and without transmitter IQI compensation. Secondly, this choice of $\mathbf{W}_{RF}$ can be directly computed by using singular value decomposition (SVD) of the channel matrix $\mathbf{H}$, thereby avoiding high computational delays and complexity associated with the typically used iterative algorithms for computing $\mathbf{W}_{RF}$ [17]. Finally, closed-form expressions for the large antenna regime

can be derived which provide further insights regarding the dependence of R_{sum}^{WC} on the IQI parameters.

Lemma 3: In the large antenna limit, $\mathbf{W}_{RF}^{opt}$ *satisfies*

$$\lim_{N\to\infty} (\mathbf{W}_{RF}^{opt})^H (\mathbf{W}_{RF}^{opt}) = \mathbf{I}_K \tag{23}$$

$$\text{and} \quad \lim_{N\to\infty} \mathbf{U}^H \mathbf{W}_{RF}^{opt} = \frac{\sqrt{\pi}}{2} \left[\mathbf{I}_K \ \mathbf{0}_{K\times(N-K)}\right]^T. \tag{24}$$

Proof: Please see Appendix C. ■

Lemma 3 shows the asymptotic properties of $\mathbf{W}_{RF}^{opt}$ applicable in the large antenna limit. In the following Theorem 1, we use these properties to derive an approximate closed-form expression of R_{sum}^{WC} given in (17) for the large antenna regime, when the RF combiner of Lemma 2 is used (see (22)), i.e., $\mathbf{W}_{RF} = \mathbf{W}_{RF}^{opt}$.

Theorem 1: When $N_{RF} = K$*, uncorrelated Rayleigh fading, and the RF combiner of Lemma 2 are considered,* R_{sum}^{WC} *of* (17) *can be approximated in the large antenna regime as*

$$R_{sum,K}^{WC} \approx \sum_{k=1}^{K} \log_2 \left(1 + \left(\frac{\rho_u \pi N}{4\sigma_n^2}\right)\left(\frac{2g_{T,k}^2 \cos^2\phi_{T,k}}{1+g_{T,k}^2}\right)\right), \tag{25}$$

where $R_{sum,K}^{WC}$ *is the UL achievable sum-rate* R_{sum}^{WC} *for the* $N_{RF} = K$ *scenario.*

Proof: Please see Appendix D. ■

Next, we discuss some important and useful insights provided by the expression in (25).

Corollary 1: When there is no transmitter IQI at the UEs, i.e., $g_{T,k} = 1$ *and* $\phi_{T,k} = 0^\circ \ \forall k$, (25) *simplifies to*

$$R_{sum,K}^{WC} \approx K \log_2 \left(1 + \left(\frac{\rho_u \pi N}{4\sigma_n^2}\right)\right). \tag{26}$$

Corollary 1 provides the sum-rate expression of the proposed transmitter IQI compensated massive MU-MIMO HBFS for the large antenna regime when there is no IQI. It is interesting to observe that the expression in (26) is same as the sum-rate expression of the IQI-free massive MU-MIMO HBFS for the large antenna regime where no IQI compensation algorithm has been applied, which is given by

$$R_{sum,K}^{NoIQI} \approx K \log_2 \left(1 + \left(\frac{\rho_u \pi N}{4\sigma_n^2}\right)\right), \tag{27}$$

and can be easily derived from (8) and (9) by using $\mathbf{G}_1 = \mathbf{I}_K$, $\mathbf{G}_2 = \mathbf{0}_{K\times K}$, $\mathbf{W}_{BB} = \mathbf{I}_K$ and the asymptotically optimal $\mathbf{W}_{RF}$ of (22). Hence, for the no IQI scenario and large antenna regime, the performance of the massive MU-MIMO HBFS with the proposed transmitter IQI compensation approaches the performance of the massive MU-MIMO HBFS with no IQI and no compensation, i.e., the proposed compensation does not result in any rate loss when there is no IQI. This implies that the proposed transmitter IQI compensation algorithm implemented at the BS receiver does not need to specially handle the scenario when there is no IQI. This is unlike the IQI compensation algorithm proposed for FD massive MU-MIMO systems in [32] where the IQI compensation matrix $\mathbf{\Phi}_{comp}$ (see equation (32) in [32]) cannot be applied for the no IQI scenario since $\mathbf{\Phi}_{comp}$ depends on $\widehat{\mathbf{K}}_2^{-1}$; and $\widehat{\mathbf{K}}_2$ is a nearly zero matrix for the no IQI scenario.

However, when transmitter IQI is present, the difference between $R_{sum,K}^{NoIQI}$ and $R_{sum,K}^{WC}$ (see (25)) in the high SNR and large antenna regime can be approximated as

$$R_{sum,K}^{NoIQI} - R_{sum,K}^{WC} \approx \sum_{k=1}^{K} \log_2 \left(\frac{1+g_{T,k}^2}{2g_{T,k}^2 \cos^2\phi_{T,k}}\right). \tag{28}$$

From (28), it is clear that the difference between achievable sum-rate for the no IQI scenario and that with the proposed transmitter IQI compensation, is a constant which only depends on the transmitter IQI parameters and the number of users, and is independent of the number of BS antennas, transmit power and the channel matrix. Next, we examine the individual effects of amplitude mismatch and phase mismatch on the sum-rate expression given by (25).

Corollary 2: When there is only amplitude mismatch at the UEs (no phase mismatch), i.e., $g_{T,k} \neq 1$ *and* $\phi_{T,k} = 0^\circ \ \forall k$, (25) *simplifies to*

$$R_{sum,K}^{WC} \approx \sum_{k=1}^{K} \log_2 \left(1 + \left(\frac{\rho_u \pi N}{4\sigma_n^2}\right)\left(\frac{2g_{T,k}^2}{1+g_{T,k}^2}\right)\right), \tag{29}$$

and hence,

$$R_{sum,K}^{NoIQI} - R_{sum,K}^{WC} \approx \sum_{k=1}^{K} \log_2 \left(\frac{1+g_{T,k}^2}{2g_{T,k}^2}\right). \tag{30}$$

Corollary 2 shows the effect of amplitude mismatch on the sum-rate expression of (25). Particularly, it can be deduced from (30) that when $g_{T,k} > 1$, $R_{sum,K}^{NoIQI} - R_{sum,K}^{WC} < 0$ which implies that $R_{sum,K}^{WC} > R_{sum,K}^{NoIQI}$, which shows that the sum-rate obtained after applying the proposed transmitter IQI compensation algorithm can be slightly larger than the sum-rate for the no IQI scenario. Similarly, when $g_{T,k} < 1$, $R_{sum,K}^{WC} < R_{sum,K}^{NoIQI}$, which shows that the sum-rate obtained after applying the proposed transmitter IQI compensation algorithm can be slightly smaller than the sum-rate for the no IQI scenario.

Corollary 3: When there is only phase mismatch at the UEs (no amplitude mismatch), i.e., $g_{T,k} = 1$ *and* $\phi_{T,k} \neq 0^\circ \ \forall k$, (25) *simplifies to*

$$R_{sum,K}^{WC} \approx \sum_{k=1}^{K} \log_2 \left(1 + \left(\frac{\rho_u \pi N}{4\sigma_n^2}\right)\cos^2\phi_{T,k}\right), \tag{31}$$

and hence,

$$R_{sum,K}^{NoIQI} - R_{sum,K}^{WC} \approx \sum_{k=1}^{K} \log_2 \left(\frac{1}{\cos^2\phi_{T,k}}\right). \tag{32}$$

Corollary 3 explains the effect of phase mismatch on the sum-rate expression of (25). From (32), it can be concluded that, since $0 < \cos^2\phi_{T,k} \leq 1$ we have $R_{sum,K}^{NoIQI} - R_{sum,K}^{WC} > 0$ and therefore, $R_{sum,K}^{WC} < R_{sum,K}^{NoIQI}$. It shows that if phase mismatch is present, then, in the large antenna regime, the sum-rate obtained after applying the proposed transmitter

IQI compensation algorithm is always slightly smaller than the sum-rate for the no IQI scenario. As the phase mismatch increases, the difference between $R_{sum,K}^{NoIQI}$ and $R_{sum,K}^{WC}$ also increases because of the decreasing behavior of $\cos^2(\phi_{T,k})$ with increasing magnitude of the phase mismatch, i.e., $|\phi_{T,k}|$.

2) PERFORMANCE ANALYSIS FOR $N_{RF} = 2K$ SCENARIO

In this section, firstly, we present the optimal design of $\mathbf{W}_{RF}$ and $\mathbf{W}_{BB}$ for the $N_{RF} = 2K$ scenario such that the hybrid combining matrix ($\mathbf{W}_{RF}\mathbf{W}_{BB}$) becomes equal to the optimal FD combining matrix. Secondly, we derive an approximate closed-form expression of R_{sum}^{WC} given in (17) for the large antenna regime and uncorrelated Rayleigh fading.

Lemma 4: For the $N_{RF} = 2K$ scenario, the optimal hybrid combining matrices $\mathbf{W}_{RF}$ and $\mathbf{W}_{BB}$ which satisfy $\mathbf{W}_{RF}\mathbf{W}_{BB} = \mathbf{U}_{1:K}$ are given by

$$[\mathbf{W}_{RF}^{opt}]_{n,p} = \begin{cases} \frac{1}{\sqrt{N}} e^{j\left(\angle U_{n,k} + \cos^{-1}(|U_{n,k}|)\right)} & \text{for } p = 2k-1, \\ \frac{1}{\sqrt{N}} e^{j\left(\angle U_{n,k} - \cos^{-1}(|U_{n,k}|)\right)} & \text{for } p = 2k, \end{cases}$$
$$\mathbf{W}_{BB}^{opt} = (\sqrt{N}/2)\, diag\{\mathbf{1}_{2\times 1}, \ldots, \mathbf{1}_{2\times 1}\}, \tag{33}$$

where $n \in \{1, 2, \ldots, N\}$ and $k \in \{1, 2, \ldots, K\}$.

Proof: Please see Appendix E. ∎

Next, we derive an approximate closed-form expression of R_{sum}^{WC} given in (17) for the large antenna regime when the hybrid combining matrices given in Lemma 4 are used, i.e., $\mathbf{W}_{RF} = \mathbf{W}_{RF}^{opt}$ and $\mathbf{W}_{BB} = \mathbf{W}_{BB}^{opt}$.

Theorem 2: When $N_{RF} = 2K$, uncorrelated Rayleigh fading, and the RF combiner of Lemma 4 are considered, R_{sum}^{WC} of (17) can be approximated in the large antenna regime as

$$R_{sum,2K}^{WC} \approx \sum_{k=1}^{K} \log_2\left(1 + \left(\frac{\rho_u N}{\sigma_n^2}\right)\left(\frac{2g_{T,k}^2 \cos^2\phi_{T,k}}{1 + g_{T,k}^2}\right)\right), \tag{34}$$

where $R_{sum,2K}^{WC}$ is the UL achievable sum-rate R_{sum}^{WC} for $N_{RF} = 2K$ scenario.

Proof: Please see Appendix F. ∎

Similar to the $N_{RF} = K$ scenario, next, we discuss the insights provided by $R_{sum,2K}^{WC}$, which are given below.

Corollary 4: When there is no transmitter IQI at the UEs, (34) simplifies to

$$R_{sum,2K}^{NoIQI} \approx K \log_2\left(1 + \left(\frac{\rho_u N}{\sigma_n^2}\right)\right). \tag{35}$$

Corollary 4 provides the asymptotic sum-rate expression for the case when there is no IQI and $N_{RF} = 2K$. Hence, from (34) and (35), the difference between $R_{sum,2K}^{NoIQI}$ and $R_{sum,2K}^{WC}$ in the high SNR and large antenna regime can be approximated as

$$R_{sum,2K}^{NoIQI} - R_{sum,2K}^{WC} \approx \sum_{k=1}^{K} \log_2\left(\frac{1 + g_{T,k}^2}{2g_{T,k}^2 \cos^2\phi_{T,k}}\right). \tag{36}$$

We observe that the expressions in the right hand side (R.H.S.) of (28) and (36) are the same, which shows that the difference between achievable sum-rates for the no IQI scenario and that with the proposed transmitter IQI compensation is the same for $N_{RF} = K$ and $N_{RF} = 2K$ scenarios. Next, we examine the individual effects of amplitude mismatch and phase mismatch on the sum-rate expression given by (34).

Corollary 5: When there is only amplitude mismatch at the UEs (no phase mismatch), (34) simplifies to

$$R_{sum,2K}^{WC} \approx \sum_{k=1}^{K} \log_2\left(1 + \left(\frac{\rho_u N}{\sigma_n^2}\right)\left(\frac{2g_{T,k}^2}{1 + g_{T,k}^2}\right)\right), \tag{37}$$

and hence,

$$R_{sum,2K}^{NoIQI} - R_{sum,2K}^{WC} \approx \sum_{k=1}^{K} \log_2\left(\frac{1 + g_{T,k}^2}{2g_{T,k}^2}\right). \tag{38}$$

Corollary 6: When there is only phase mismatch at the UEs (no amplitude mismatch), (34) simplifies to

$$R_{sum,2K}^{WC} \approx \sum_{k=1}^{K} \log_2\left(1 + \left(\frac{\rho_u N}{\sigma_n^2}\right)\cos^2\phi_{T,k}\right), \tag{39}$$

and hence,

$$R_{sum,2K}^{NoIQI} - R_{sum,2K}^{WC} \approx \sum_{k=1}^{K} \log_2\left(\frac{1}{\cos^2\phi_{T,k}}\right). \tag{40}$$

We observe that the expressions in the R.H.S. of (38) and (40) are the same as the expressions given in the R.H.S. of (30) and (32), respectively, because of which the insights provided by Corollaries 5 and 6 (for $N_{RF} = 2K$ scenario) are the same as those provided by Corollaries 2 and 3 (for $N_{RF} = K$ scenario).

In the next section, we provide the approximate UL achievable sum-rate of the transmitter IQI compensated UL massive MU-MIMO HBFS for the general scenario $K \le N_{RF} \le 2K$, which is based on combining the results obtained for $N_{RF} = K$ and $N_{RF} = 2K$ scenarios.

3) PERFORMANCE ANALYSIS FOR $K \le N_{RF} \le 2K$ SCENARIO

For the $K \le N_{RF} \le 2K$ scenario, the hybrid combining matrices are designed by properly choosing the combining vectors from the hybrid combining matrices for $N_{RF} = K$ and $N_{RF} = 2K$ scenarios, and then, an approximate closed-form expression of R_{sum}^{WC} given in (17) for the large antenna regime is derived which is based on the results of Theorem 1 and Theorem 2.

Lemma 5: For the $K \le N_{RF} \le 2K$ scenario, the asymptotically optimal hybrid combining matrices $\mathbf{W}_{RF}$ and $\mathbf{W}_{BB}$ are given by

$$[\mathbf{W}_{RF}^{opt}]_{n,p} = \begin{cases} \frac{1}{\sqrt{N}} e^{j\left(\angle U_{n,k_1} + \cos^{-1}(|U_{n,k_1}|)\right)} & \text{for } p = 2k_1 - 1, \\ \frac{1}{\sqrt{N}} e^{j\left(\angle U_{n,k_1} - \cos^{-1}(|U_{n,k_1}|)\right)} & \text{for } p = 2k_1, \\ \frac{1}{\sqrt{N}} e^{j\angle U_{n,k_2}} & \text{for } p = k_2, \end{cases}$$
$$\mathbf{W}_{BB}^{opt} = diag\left((\sqrt{N}/2)(\mathbf{I}_{N_{RF}-K} \otimes \mathbf{1}_{2\times 1}), \mathbf{I}_{2K-N_{RF}}\right), \tag{41}$$

where $n \in \{1, 2, \ldots, N\}$, $k_1 \in \{1, 2, \ldots, (N_{RF} - K)\}$, *and* $k_2 \in \{(2(N_{RF} - K) + 1), \ldots, N_{RF}\}$.

Proof: Please see Appendix G. ∎

Next, we present an approximate closed-form expression of R_{sum}^{WC} given in (17) for the large antenna regime which is applicable for any choice of N_{RF} where $K \leq N_{RF} \leq 2K$, when the hybrid combining matrices given in Lemma 5 are used.

Theorem 3: When $K \leq N_{RF} \leq 2K$, *uncorrelated Rayleigh fading, and the RF combiner of Lemma 5 are considered,* R_{sum}^{WC} *of* (17) *can be approximated in the large antenna regime as*

$$R_{sum}^{WC} \approx \sum_{k=1}^{N_{RF}-K} \log_2\left(1 + \left(\frac{\rho_u N}{\sigma_n^2}\right)\left(\frac{2g_{T,k}^2 \cos^2\phi_{T,k}}{1 + g_{T,k}^2}\right)\right) + \sum_{k=N_{RF}-K+1}^{K} \log_2\left(1 + \left(\frac{\rho_u \pi N}{4\sigma_n^2}\right)\left(\frac{2g_{T,k}^2 \cos^2\phi_{T,k}}{1 + g_{T,k}^2}\right)\right). \quad (42)$$

Proof: Please see Appendix H. ∎

From Theorem 3, it can be deduced that for a massive MU-MIMO HBFS serving K UEs with N_{RF} RF chains; the extra $(N_{RF} - K)$ RF chains are used to provide optimal FD performance for $(N_{RF} - K)$ UEs, while the remaining $(2K - N_{RF})$ RF chains are used to provide hybrid beamforming performance for the remaining $(2K - N_{RF})$ UEs. Next, we discuss the insights provided by the closed-form expression given in (42) for the general $K \leq N_{RF} \leq 2K$ scenario.

Corollary 7: When there is no transmitter IQI at the UEs, (42) *simplifies to*

$$R_{sum}^{NoIQI} \approx (N_{RF} - K)\log_2\left(1 + \left(\frac{\rho_u N}{\sigma_n^2}\right)\right) + (2K - N_{RF})\log_2\left(1 + \left(\frac{\rho_u \pi N}{4\sigma_n^2}\right)\right). \quad (43)$$

Corollary 7 provides the asymptotic sum-rate expression for the case when there is no IQI and $K \leq N_{RF} \leq 2K$. Hence, from (42) and (43), the difference between R_{sum}^{NoIQI} and R_{sum}^{WC} in the high SNR and large antenna regime can be approximated as

$$R_{sum}^{NoIQI} - R_{sum}^{WC} \approx \sum_{k=1}^{N_{RF}-K} \log_2\left(\frac{1 + g_{T,k}^2}{2g_{T,k}^2 \cos^2\phi_{T,k}}\right) + \sum_{k=N_{RF}-K+1}^{K} \log_2\left(\frac{1 + g_{T,k}^2}{2g_{T,k}^2 \cos^2\phi_{T,k}}\right) = \sum_{k=1}^{K} \log_2\left(\frac{1 + g_{T,k}^2}{2g_{T,k}^2 \cos^2\phi_{T,k}}\right). \quad (44)$$

We observe that the simplified expression in (44) for the $K \leq N_{RF} \leq 2K$ scenario is same as the corresponding expressions for $N_{RF} = K$ and $N_{RF} = 2K$ scenarios (see (28) and (36)). Hence, the difference between achievable sum-rate for the no IQI scenario and that with the proposed transmitter IQI compensation is also *independent* of the number of RF chains at the BS.

Corollary 8: When there is only amplitude mismatch at the UEs (no phase mismatch), (42) *simplifies to*

$$R_{sum}^{WC} \approx \sum_{k=1}^{N_{RF}-K} \log_2\left(1 + \left(\frac{\rho_u N}{\sigma_n^2}\right)\left(\frac{2g_{T,k}^2}{1 + g_{T,k}^2}\right)\right) + \sum_{k=N_{RF}-K+1}^{K} \log_2\left(1 + \left(\frac{\rho_u \pi N}{4\sigma_n^2}\right)\left(\frac{2g_{T,k}^2}{1 + g_{T,k}^2}\right)\right), \quad (45)$$

and hence,

$$R_{sum}^{NoIQI} - R_{sum}^{WC} \approx \sum_{k=1}^{K} \log_2\left(\frac{1 + g_{T,k}^2}{2g_{T,k}^2}\right), \quad (46)$$

where (46) is found to be equal to the expressions given in (30) and (38).

Corollary 9: When there is only phase mismatch at the UEs (no amplitude mismatch), (42) *simplifies to*

$$R_{sum}^{WC} \approx \sum_{k=1}^{N_{RF}-K} \log_2\left(1 + \left(\frac{\rho_u N}{\sigma_n^2}\right)\cos^2\phi_{T,k}\right) + \sum_{k=N_{RF}-K+1}^{K} \log_2\left(1 + \left(\frac{\rho_u \pi N}{4\sigma_n^2}\right)\cos^2\phi_{T,k}\right), \quad (47)$$

and hence,

$$R_{sum}^{NoIQI} - R_{sum}^{WC} \approx \sum_{k=1}^{K} \log_2\left(\frac{1}{\cos^2\phi_{T,k}}\right), \quad (48)$$

where (48) is found to be equal to the expressions given in (32) and (40).

IV. NUMERICAL RESULTS

In this section, we provide numerical results to evaluate the sum-rate performance of the UL massive MU-MIMO HBFS with transmitter IQI for the following two cases: (i) when the transmitter IQI compensation is not performed, (ii) when the proposed transmitter IQI compensation algorithm has been applied at the BS. For bench-marking and comparison, the performance of the IQI-free FD massive MU-MIMO system and the IQI-free massive MU-MIMO HBFS is also discussed. The average UL achievable sum-rate is calculated by averaging over independent and random realizations of the channel matrix $\mathbf{H}$ and the transmitter IQI parameters $\{g_k\}_{k=1}^K$, $\{\phi_k\}_{k=1}^K$. The IQI parameters g_k and ϕ_k are assumed to be uniformly distributed in an interval which is centered around their ideal values (the ideal values of g_k and ϕ_k for no IQI scenario are 1 and 0° respectively), i.e., $g_k \sim Unif[1 - \delta_g, 1 + \delta_g]$ and $\phi_k \sim Unif[-\delta_\phi, \delta_\phi]$, where δ_g and δ_ϕ, respectively, denote the deviations in g_k and ϕ_k from their ideal values [37].

To show the effectiveness of the proposed transmitter IQI compensation algorithm in different propagation environments, we consider three different channel models, namely, (i) uncorrelated Rayleigh fading channels, (ii) correlated

Rayleigh fading channels, and (iii) sparse mm-wave channels. For uncorrelated Rayleigh fading channels, each entry of $\mathbf{H}$ is modeled as i.i.d. ZMCSCG random variable with variance 1, i.e., $[\mathbf{H}]_{n,k} \sim \mathcal{CN}(0,1)$, whereas for correlated Rayleigh fading channels, $\mathbf{H} = \mathbf{R}^{1/2}\mathbf{H}_u$ is considered where $\mathbf{H}_u \in \mathbb{C}^{N\times K}$ models the uncorrelated Rayleigh fading channel and $\mathbf{R} \in \mathbb{C}^{N\times N}$ models the spatial correlation at the BS [24]. Assuming an exponentially correlated channel model, $\mathbf{R}$ is given by [51], [52]

$$\mathbf{R} = \begin{bmatrix} 1 & r & \dots & r^{N-1} \\ r & 1 & \dots & r^{N-2} \\ \vdots & \vdots & \ddots & \vdots \\ r^{N-1} & r^{N-2} & \dots & 1 \end{bmatrix}, \tag{49}$$

where $0 \le r \le 1$ is the correlation coefficient, and the cases $r = 0$ and $r = 1$ correspond to no correlation and perfect correlation scenarios, respectively. Finally, for the sparse mm-wave channel, $\mathbf{H} \triangleq [\mathbf{h}_1, \mathbf{h}_2, \dots, \mathbf{h}_K]$, where $\mathbf{h}_k \in \mathbb{C}^{N\times 1}$ is the channel vector between the k^{th} UE and the BS antennas $\forall\, k \in \{1, 2, \dots, K\}$. We assume that $\mathbf{h}_k$ follows a narrow-band clustered channel model having L propagation paths and is given by [24], [43]

$$\mathbf{h}_k = \sqrt{\frac{N}{L}} \sum_{l=1}^{L} \alpha_{l,k}\, \mathbf{a}_r(\phi_{l,k}), \tag{50}$$

where $\alpha_{l,k} \sim \mathcal{CN}(0,1)$ is the complex gain of the l^{th} multipath of the k^{th} UE for $l \in \{1, 2, \dots, L\}$ and $k \in \{1, 2, \dots, K\}$, and $\mathbf{a}_r(\phi_{l,k}) \in \mathbb{C}^{N\times 1}$ is the array response vector of the BS in the direction $\phi_{l,k}$ ($\phi_{l,k} \sim Unif[0, \pi]$ is the angle of arrival of the l^{th} multipath for the k^{th} UE) and is expressed as

$$\mathbf{a}_r(\phi_{l,k}) = \frac{1}{\sqrt{N}} \left[1, e^{jkd\sin(\phi_{l,k})}, \dots, e^{jkd(N-1)\sin(\phi_{l,k})}\right]^T, \tag{51}$$

where $k \triangleq 2\pi/\lambda$, λ is the wavelength of the carrier signal, and $d = \lambda/2$ is the inter-element spacing (we have assumed a uniform linear array at the BS). The noise variance σ_n^2 is assumed to be equal to 1 due to which ρ_u can be interpreted as the transmit SNR. In all the figures, 'C_{sum}^{NoIQI}' represents the UL achievable sum-rate of the IQI-free FD massive MU-MIMO system, '$R_{sum,K}^{NC}$' and '$R_{sum,2K}^{NC}$' denote the UL sum-rates achieved by the transmitter IQI uncompensated massive MU-MIMO HBFSs for $N_{RF} = K$ and $N_{RF} = 2K$ scenarios, respectively, whereas 'R_{sum}^{NoIQI}', '$R_{sum,K}^{NoIQI}$', '$R_{sum,2K}^{NoIQI}$', 'R_{sum}^{WC}', '$R_{sum,K}^{WC}$', '$R_{sum,2K}^{WC}$', 'R_{sum}^{NC}', and '$R_{sum,ceil}^{NC}$' are defined in the previous section.

Considering uncorrelated Rayleigh fading, we plot the approximate UL achievable sum-rate provided by the closed-form expressions of (25), (34), and (42) along with the exact UL achievable sum-rate obtained by numerical simulation (see (17)). After discussing the performance of different massive MU-MIMO HBFSs in uncorrelated Rayleigh fading, we also provide the sum-rate plots for the correlated Rayleigh fading channel and sparse mm-wave channel.

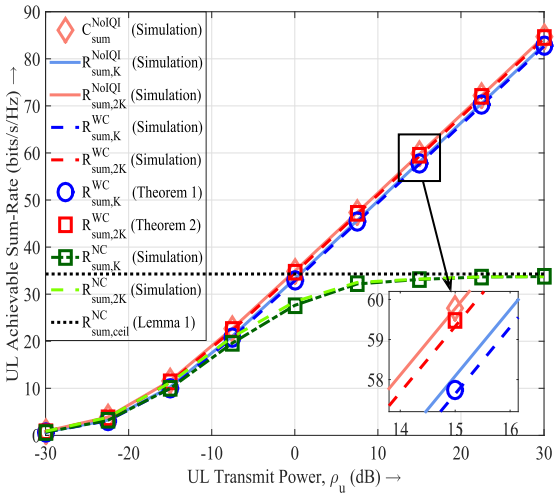

FIGURE 2. UL achievable sum-rate (bits/s/Hz) of different massive MU-MIMO HBFSs as a function of ρ_u for uncorrelated Rayleigh fading channel, $N = 128$, $K = 5$, $\delta_g = 0.2$, and $\delta_\phi = 20°$.

In Fig. 2, considering uncorrelated Rayleigh fading, we plot the average UL achievable sum-rate as a function of the UL transmit power ρ_u for the scenario where the number of antennas at the BS is $N = 128$, the number of UEs in the cell using the same time-frequency resource is $K = 5$, the deviation of the amplitude mismatch parameter is $\delta_g = 0.2$, and the deviation of the phase mismatch parameter is $\delta_\phi = 20°$. We observe that C_{sum}^{NoIQI}, $R_{sum,K}^{NoIQI}$ and $R_{sum,2K}^{NoIQI}$ increase unboundedly with increasing ρ_u and the plot of $R_{sum,2K}^{NoIQI}$ coincides with the plot of C_{sum}^{NoIQI} for all values of ρ_u whereas the plot of $R_{sum,K}^{NoIQI}$ lies slightly lower than the plots of $R_{sum,2K}^{NoIQI}$ and C_{sum}^{NoIQI}. This confirms that the sum-rate performance of HBFSs with $N_{RF} = 2K$ is equal to the sum-rate performance of an FD system whereas a HBFS with $N_{RF} = K$ achieves slightly smaller sum-rate than a HBFS with $N_{RF} = 2K$. Furthermore, in contrast to the sum-rate performance of the above IQI-free HBFSs, $R_{sum,K}^{NC}$ and $R_{sum,2K}^{NC}$ ceil at the higher values of ρ_u and their maximum possible value is given by $R_{sum,ceil}^{NC}$. This shows that if the transmitter IQI is not compensated, a high sum-rate cannot be achieved, and hence transmitter IQI compensation is required for UL massive MU-MIMO HBFS. However, after applying the proposed transmitter IQI compensation algorithm, it is observed that both $R_{sum,K}^{WC}$ and $R_{sum,2K}^{WC}$ increase unboundedly with ρ_u and are almost equal to $R_{sum,K}^{NoIQI}$ and $R_{sum,2K}^{NoIQI}$, respectively. This confirms that the proposed transmitter IQI compensation algorithm efficiently mitigates the undesired effects of transmitter IQI. Also, the approximate values of $R_{sum,K}^{WC}$ and $R_{sum,2K}^{WC}$ given by Theorem 1 and Theorem 2, respectively, match with the exact values of $R_{sum,K}^{WC}$ and $R_{sum,2K}^{WC}$ obtained by numerical simulation of (17).

In Fig. 3, considering uncorrelated Rayleigh fading, we plot the average UL achievable sum-rate as a function of the number of BS antennas N for the scenario where $\rho_u = 5$ dB,

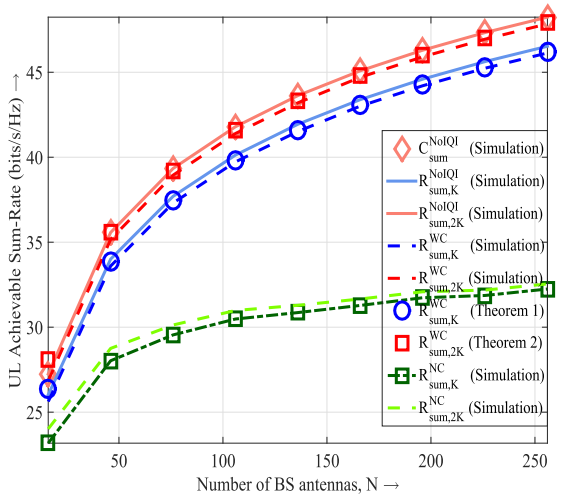

FIGURE 3. UL achievable sum-rate (bits/s/Hz) of different massive MU-MIMO HBFSs as a function of N for uncorrelated Rayleigh fading channel, $\rho_u = 5$ dB, $K = 5$, $\delta_g = 0.2$, and $\delta_\phi = 20°$.

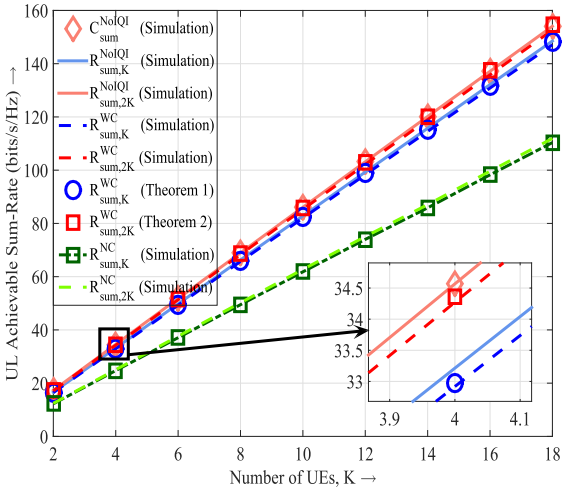

FIGURE 4. UL achievable sum-rate (bits/s/Hz) of different massive MU-MIMO HBFSs as a function of K for uncorrelated Rayleigh fading channel, $\rho_u = 5$ dB, $N = 128$, $\delta_g = 0.2$, and $\delta_\phi = 20°$.

$K = 5$, $\delta_g = 0.2$, and $\delta_\phi = 20°$. We observe that as N increases, the difference between R_{sum}^{NoIQI} and R_{sum}^{NC} also increases for both $N_{RF} = K$ and $N_{RF} = 2K$ scenarios. This shows that if the transmitter IQI is left uncompensated in the massive MU-MIMO HBFS, then only increasing the number of BS antennas does not provide resilience against the transmitter IQI. However, after applying the proposed transmitter IQI compensation algorithm, R_{sum}^{WC} is nearly equal to R_{sum}^{NoIQI} for both $N_{RF} = K$ and $N_{RF} = 2K$ scenarios. Also, the simulation and approximation of R_{sum}^{WC} match for both $N_{RF} = K$ and $N_{RF} = 2K$ scenarios. This again shows the effectiveness of the proposed transmitter IQI compensation algorithm and the accuracy of large antenna approximation of the UL sum-rate achieved by the massive MU-MIMO HBFS with the proposed transmitter IQI compensation algorithm.

In Fig. 4, considering uncorrelated Rayleigh fading, we plot the average UL achievable sum-rate as a function of the number of UEs K for the scenario where $\rho_u = 5$ dB, $N = 128$, $\delta_g = 0.2$, and $\delta_\phi = 20°$. We observe that as K increases, for both $N_{RF} = K$ and $N_{RF} = 2K$ scenarios, R_{sum}^{NC} along with C_{sum}^{NoIQI}, R_{sum}^{NoIQI}, and R_{sum}^{WC} also increases which is because of the increasing number of UEs. However, the difference between R_{sum}^{NoIQI} and R_{sum}^{NC}, for both $N_{RF} = K$ and $N_{RF} = 2K$ scenarios, increases with increasing K. This shows that the sum-rate performance of a transmitter IQI uncompensated massive MU-MIMO HBFS deviates from the optimal sum-rate performance of an IQI-free massive MU-MIMO HBFS when more UEs are scheduled. Also, this observation is in agreement with the results of (28), (36), and (44). Meanwhile, after applying the proposed transmitter IQI compensation algorithm, the plots of R_{sum}^{WC} are almost equal to R_{sum}^{NoIQI} for both $N_{RF} = K$ and $N_{RF} = 2K$ scenarios.

In Fig. 5, considering uncorrelated Rayleigh fading, the average UL achievable sum-rate is plotted as a function of the amplitude deviation δ_g for the case when $\rho_u = 5$ dB, $N = 128$, $K = 5$, and $\delta_\phi = 0°$. This setting particularly

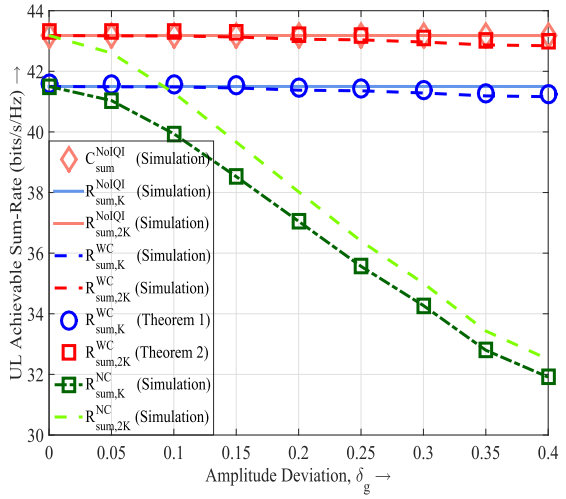

FIGURE 5. UL achievable sum-rate (bits/s/Hz) of different massive MU-MIMO HBFSs as a function of δ_g for uncorrelated Rayleigh fading channel, $\rho_u = 5$ dB, $N = 128$, $K = 5$, and $\delta_\phi = 0°$.

examines the effect of amplitude mismatch on the average UL achievable sum-rate of the transmitter IQI impaired massive MU-MIMO HBFS with and without IQI compensation. We observe that the plots of C_{sum}^{NoIQI}, $R_{sum,K}^{NoIQI}$, and $R_{sum,2K}^{NoIQI}$ are constant. This is because by definition, these systems are IQI-free and hence are independent of δ_g. In contrast, both $R_{sum,K}^{NC}$ and $R_{sum,2K}^{NC}$ decrease with increasing δ_g. For example, when $\delta_g = 0.2$, $R_{sum,K}^{NC}$ is about 37 bits/s/Hz as compared to $R_{sum,K}^{NoIQI}$ which is about 41.5 bits/s/Hz. Also, for severe amplitude mismatch, i.e., when $\delta_g = 0.4$, $R_{sum,K}^{NC}$ further reduces to about 32 bits/s/Hz. This is because increasing values of δ_g results in more amplitude mismatch which subsequently decreases the achievable sum-rate. However, with the proposed transmitter IQI compensation and for both $N_{RF} = K$ and $N_{RF} = 2K$ scenarios, R_{sum}^{WC} (both exact and approximate) are close to R_{sum}^{NoIQI} for a wide range of δ_g. However, a small

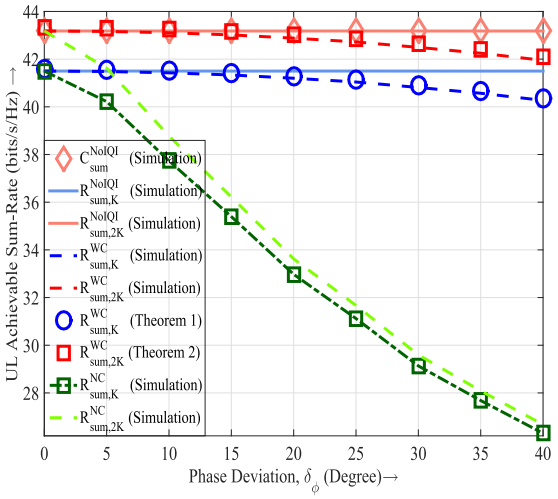

FIGURE 6. UL achievable sum-rate (bits/s/Hz) of different massive MU-MIMO HBFSs as a function of δ_ϕ for uncorrelated Rayleigh fading channel, $\rho_u = 5$ dB, $N = 128$, $K = 5$, and $\delta_g = 0$.

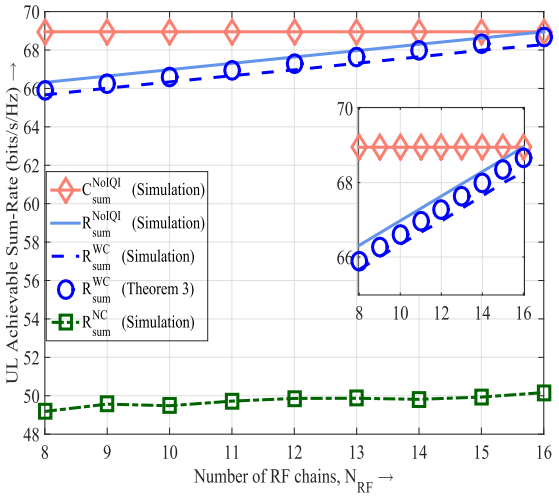

FIGURE 7. UL achievable sum-rate (bits/s/Hz) of different massive MU-MIMO HBFSs as a function of N_{RF} for uncorrelated Rayleigh fading channel, $\rho_u = 5$ dB, $N = 128$, $K = 8$, $\delta_g = 0.2$, and $\delta_\phi = 20°$.

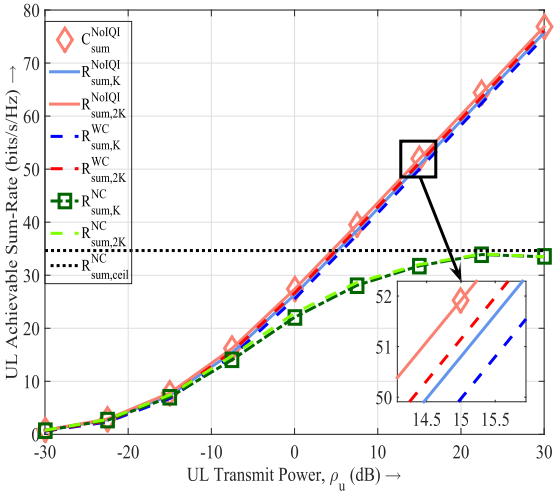

FIGURE 8. UL achievable sum-rate (bits/s/Hz) of different massive MU-MIMO HBFSs as a function of ρ_u for correlated Rayleigh fading channel, $r = 0.99$, $N = 128$, $K = 5$, $\delta_g = 0.2$, and $\delta_\phi = 20°$.

degradation is observed in R_{sum}^{WC} when compared to R_{sum}^{NoIQI}, only when the amplitude mismatch is severe. This support the observations made in Corollary 2 and Corollary 5. Therefore the proposed transmitter IQI compensation algorithm effectively mitigates the performance degradation caused by severe amplitude mismatch in massive MU-MIMO HBFSs.

In Fig. 6, for uncorrelated Rayleigh fading, the average UL achievable sum-rate is plotted as a function of the phase deviation δ_ϕ when $\rho_u = 5$ dB, $N = 128$, $K = 5$, and $\delta_g = 0$. This setting particularly examines the effect of phase mismatch on the average UL achievable sum-rate of the transmitter IQI impaired massive MU-MIMO HBFS with and without IQI compensation. Similar to Fig. 5, it is observed that the plots of C_{sum}^{NoIQI}, $R_{sum,K}^{NoIQI}$, and $R_{sum,2K}^{NoIQI}$ are independent of δ_ϕ and hence are constant. The plots of both $R_{sum,K}^{NC}$ and $R_{sum,2K}^{NC}$ decrease with increasing δ_ϕ since larger values of δ_ϕ result in more phase mismatch which subsequently decreases the achievable sum-rate. However, with the proposed transmitter IQI compensation and for both $N_{RF} = K$ and $N_{RF} = 2K$ scenarios, R_{sum}^{WC} (both exact and approximate) is nearly same as R_{sum}^{NoIQI} for a wide range of δ_ϕ. For severe phase mismatch, a small gap is observed in the plots of R_{sum}^{WC} when compared with R_{sum}^{NoIQI}. The reason for this gap is explained in Corollary 3 and Corollary 6. This shows that the proposed transmitter IQI compensation algorithm effectively mitigates the performance degradation caused by severe phase mismatch in massive MU-MIMO HBFSs.

In Fig. 7, for uncorrelated Rayleigh fading, the average UL achievable sum-rate is plotted as a function of the number of RF chains ($K \leq N_{RF} \leq 2K$) when $\rho_u = 5$ dB, $N = 128$, $K = 8$, $\delta_g = 0.2$, and $\delta_\phi = 20°$. It can be observed from Fig. 7 that, irrespective of the number of RF chains, the UL sum-rate achieved with the proposed transmitter IQI compensation is very close to the UL achievable sum-rate for the no IQI scenario. Also, the UL achievable sum-rate increases with increasing number of RF chains for both IQI-free and with IQI compensation scenarios, and the simulation and approximation of R_{sum}^{WC} closely match. Also, when $N_{RF} = 2K$, the sum-rate of FD MU-MIMO systems is achieved, which justifies that increasing N_{RF} beyond $2K$ does not bring further improvement in the performance, but the system cost and energy consumption will surely increase.

Finally, in Fig. 8 and Fig. 9, we plot the average UL achievable sum-rate as a function of ρ_u for correlated Rayleigh fading and sparse mm-wave channels, respectively, when $N = 128$, $K = 5$, $\delta_g = 0.2$, and $\delta_\phi = 20°$. We choose $r = 0.99$ and $L = 2$ to model an extremely high correlation scenario for the correlated Rayleigh fading channel and a sparse scattering scenario for the sparse mm-wave channel, respectively. We observe that in both the figures (Fig. 8 and Fig. 9) and for both $N_{RF} = K$ and $N_{RF} = 2K$ scenarios, C_{sum}^{NoIQI}, R_{sum}^{NoIQI}, and R_{sum}^{WC} increase unboundedly with increasing ρ_u whereas R_{sum}^{NC} ceils at the higher values of ρ_u. Also, R_{sum}^{WC} is almost

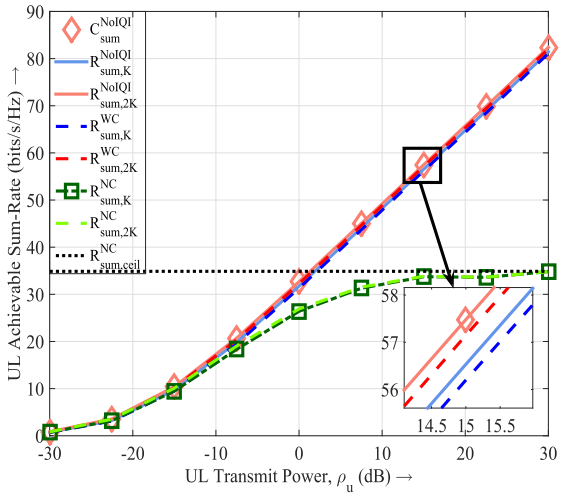

FIGURE 9. UL achievable sum-rate (bits/s/Hz) of different massive MU-MIMO HBFSs as a function of ρ_u for sparse mm-wave channel, $L = 2$, $N = 128$, $K = 5$, $\delta_g = 0.2$, and $\delta_\phi = 20°$.

equal to R_{sum}^{NoIQI} for both the channels. This confirms that the proposed transmitter IQI compensation algorithm efficiently mitigates the undesired effects of transmitter IQI in *different channel environments and is not only limited to uncorrelated Rayleigh fading channels*.

V. CONCLUSION

In this paper, we consider the UL communication of a massive MU-MIMO HBFS affected by transmitter IQI. It is shown that uncompensated transmitter IQI causes a finite ceiling of the UL achievable sum-rate at high SNR. To solve this problem, a novel ZF based transmitter IQI compensation algorithm, which effectively mitigates the undesired effects of transmitter IQI, has been proposed and is shown to be applicable for any channel model and any choice of the number of RF chains. The UL sum-rate performance analysis of the effective massive MU-MIMO HBFS with the proposed transmitter IQI compensation algorithm has been discussed and an approximate closed-form expression of the UL achievable sum-rate has been derived for the large antenna regime when the channel is modeled by uncorrelated Rayleigh fading. Simulation results show that the proposed transmitter IQI compensation algorithm effectively mitigates the undesired effects of both amplitude mismatch and phase mismatch even when different channel models are assumed.

APPENDIX A
PROOF OF LEMMA 1

By substituting the expression of $\mathbf{K}_{n_e}$ from (9) in (8), and taking the limit $\rho_u/\sigma_n^2 \to \infty$, we get,

$$\begin{aligned}\lim_{\rho_u/\sigma_n^2\to\infty} R_{sum}^{NC} &= \log_2 \det\left(\mathbf{I}_K + (\mathbf{H}_{IQ}\mathbf{H}_{IQ}^H)^{-1}\mathbf{H}_{DS}\mathbf{H}_{DS}^H\right)\\ &\overset{(a)}{=} \log_2 \det\left(\mathbf{I}_K + \mathbf{H}_{DS}^H\mathbf{H}_{IQ}^{-H}\mathbf{H}_{IQ}^{-1}\mathbf{H}_{DS}\right)\\ &\overset{(b)}{=} \log_2 \det\left(\mathbf{I}_K + \mathbf{G}_1^H\mathbf{G}_2^{-T}\mathbf{G}_2^{-*}\mathbf{G}_1\right)\\ &\overset{(c)}{=} \log_2 \det\left(\mathbf{I}_K + (\mathbf{G}_2\mathbf{G}_2^H)^{-1}\mathbf{G}_1\mathbf{G}_1^H\right), \quad (52)\end{aligned}$$

where (a) is obtained by using the Weinstein-Aronszajn identity $\det(\mathbf{I}+\mathbf{AB}) = \det(\mathbf{I}+\mathbf{BA})$, (b) is obtained by using the definitions of $\mathbf{H}_{DS}$ and $\mathbf{H}_{IQ}$, and (c) is the result of simplification performed after using the Weinstein-Aronszajn identity and exploiting the fact that $\mathbf{G}_2^H\mathbf{G}_2 = \mathbf{G}_2\mathbf{G}_2^H$ which comes from the diagonal structure of $\mathbf{G}_2$. In (a), $\mathbf{H}_{IQ}$ is invertible if and only if $\mathbf{G}_2$ has full-rank, i.e., when the RF chains of all transmitting UEs are IQ-impaired. This is because to receive the data-streams transmitted by K UEs, the BS selects $\mathbf{W}_{RF}$ and $\mathbf{W}_{BB}$ such that at least K spatial DoF are excited which gives $\text{rank}(\mathbf{W}_{BB}^H\mathbf{W}_{RF}^H\mathbf{H}) \geq K$. However, $\mathbf{W}_{BB} \in \mathbb{C}^{N_{RF}\times K}$, $\mathbf{W}_{RF} \in \mathbb{C}^{N\times N_{RF}}$, and $\mathbf{H} \in \mathbb{C}^{N\times K}$ imply that $\text{rank}(\mathbf{W}_{BB}^H\mathbf{W}_{RF}^H\mathbf{H}) \leq K$. Therefore, $\mathbf{W}_{BB}^H\mathbf{W}_{RF}^H\mathbf{H}$ has full rank, i.e., $\text{rank}(\mathbf{W}_{BB}^H\mathbf{W}_{RF}^H\mathbf{H}) = K$, and is also invertible. Hence, we arrive at the conclusion that $\mathbf{H}_{IQ} = \mathbf{W}_{BB}^H\mathbf{W}_{RF}^H\mathbf{H}\mathbf{G}_2^*$ is invertible if and only if $\mathbf{G}_2$ has full rank and hence in (a), $\mathbf{H}_{IQ}^{-1}\mathbf{H}_{DS}$ simplifies to $\mathbf{G}_2^{-*}\mathbf{G}_1$.

APPENDIX B
PROOF OF LEMMA 2

The proof follows from the proof of Lemma 5 in [17], where the asymptotically optimal precoder for the DL MU-MIMO HBFS has been derived. Following the same line of reasoning in [17], but for the UL scenario gives us (22).

APPENDIX C
PROOF OF LEMMA 3

As $[\mathbf{W}_{RF}]_{n,p} = \frac{1}{\sqrt{N}}e^{j\phi_{n,p}}$, we have each diagonal entry of $\mathbf{W}_{RF}^H\mathbf{W}_{RF}$, i.e., $[\mathbf{W}_{RF}^H\mathbf{W}_{RF}]_{p,p} = \frac{1}{N}\sum_{n=1}^{N} 1 = 1 \ \forall\ p \in \{1,2,\ldots,K\}$. However, when $\mathbf{W}_{RF} = \mathbf{W}_{RF}^{opt}$ is chosen, the off-diagonal elements of $(\mathbf{W}_{RF}^H\mathbf{W}_{RF})$, i.e., $[(\mathbf{W}_{RF}^{opt})^H(\mathbf{W}_{RF}^{opt})]_{m,p}$ for $m \neq p$, in the large antenna limit becomes $\lim_{N\to\infty}[(\mathbf{W}_{RF}^{opt})^H(\mathbf{W}_{RF}^{opt})]_{m,p} = \lim_{N\to\infty}\frac{1}{N}\sum_{n=1}^{N} e^{j(\angle U_{n,m} - \angle U_{n,p})} = \mathbb{E}\{e^{j(\angle U_{n,m} - \angle U_{n,p})}\} \overset{(a)}{=} \mathbb{E}\{e^{j\angle U_{n,m}}\}\mathbb{E}\{e^{-j\angle U_{n,p}}\} \overset{(b)}{=} \left(\frac{1}{2\pi}\int_{-\pi}^{\pi} e^{j\angle U_{n,m}} d\angle U_{n,m}\right) \times \left(\frac{1}{2\pi}\int_{-\pi}^{\pi} e^{-j\angle U_{n,p}} d\angle U_{n,p}\right) = sinc^2(1) = 0$, where, (a) follows from the statistical independence between the elements of the singular vectors of $\mathbf{H}$, and (b) follows from the fact that $U_{n,m}$ is a ZMCSCG random variable whose phase is uniformly distributed in the interval $[-\pi, \pi]$ (see Theorem 1 of [17]). Hence, $((\mathbf{W}_{RF}^{opt})^H(\mathbf{W}_{RF}^{opt}))$ becomes a square matrix with unit diagonal elements and zero off-diagonal elements, which concludes the proof of (23).

The proof of (24) follows from a similar line of reasoning as shown in Appendices A and C of [17].

APPENDIX D
PROOF OF THEOREM 1

If the RF combiner given in Lemma 2 is applied, i.e., $\mathbf{W}_{RF} = \mathbf{W}_{RF}^{opt}$, then, in the large antenna regime, $\mathbf{K}_{\widehat{n}}$ given in (21) can be simplified as

$$\mathbf{K}_{\widehat{n}} = \sigma_n^2(\mathbf{W}_{RF}^H\mathbf{H})^{-1}\mathbf{W}_{RF}^H\mathbf{W}_{RF}(\mathbf{W}_{RF}^H\mathbf{H})^{-H}$$

$$\overset{(a)}{\approx} \sigma_n^2(\mathbf{W}_{RF}^H\mathbf{H})^{-1}(\mathbf{W}_{RF}^H\mathbf{H})^{-H}$$
$$\overset{(b)}{=} \sigma_n^2(\mathbf{H}^H\mathbf{W}_{RF}\mathbf{W}_{RF}^H\mathbf{H})^{-1}, \quad (53)$$

where (a) is obtained by using (23), and (b) is obtained by using the identities $\mathbf{B}^{-1}\mathbf{A}^{-1} = (\mathbf{AB})^{-1}$ and $(\mathbf{AB})^H = \mathbf{B}^H\mathbf{A}^H$. In (53), the matrix $\mathbf{H}^H\mathbf{W}_{RF}\mathbf{W}_{RF}^H\mathbf{H}$ can be further simplified as

$$\mathbf{H}^H\mathbf{W}_{RF}\mathbf{W}_{RF}^H\mathbf{H}$$
$$\overset{(a)}{=} (\mathbf{V}\mathbf{\Sigma}^H\mathbf{U}^H\mathbf{W}_{RF})(\mathbf{V}\mathbf{\Sigma}^H\mathbf{U}^H\mathbf{W}_{RF})^H$$
$$\overset{(b)}{\approx} \left(\frac{\pi}{4}\right)\left(\mathbf{V}\mathbf{\Sigma}^H\begin{bmatrix}\mathbf{I}_K\\ \mathbf{0}_{(N-K)\times K}\end{bmatrix}\right)\left(\mathbf{V}\mathbf{\Sigma}^H\begin{bmatrix}\mathbf{I}_K\\ \mathbf{0}_{(N-K)\times K}\end{bmatrix}\right)^H$$
$$\overset{(c)}{=} \left(\frac{\pi}{4}\right)\mathbf{V}\mathbf{\Sigma}_K^H\mathbf{\Sigma}_K\mathbf{V}^H, \quad (54)$$

where (a) is obtained by using SVD of $\mathbf{H}$, i.e., $\mathbf{H} = \mathbf{U}\mathbf{\Sigma}\mathbf{V}^H$, where $\mathbf{U}$ is defined in Lemma 2, $\mathbf{V} \in \mathbb{C}^{K\times K}$ is a unitary matrix consisting of right singular vectors of $\mathbf{H}$, and $\mathbf{\Sigma} \in \mathbb{R}^{N\times K}$ contains the singular values of $\mathbf{H}$ on its diagonal elements and zeroes elsewhere. To obtain (b), we have used the result of (24), while (c) is obtained by using $\mathbf{\Sigma} = \begin{bmatrix}\mathbf{\Sigma}_K & \mathbf{0}_{K\times(N-K)}\end{bmatrix}^T$, where $\mathbf{\Sigma}_K \in \mathbb{R}^{K\times K}$ is a diagonal matrix with singular values of $\mathbf{H}$ as its diagonal elements. Further simplification of (54) is not straight-forward, hence we make an approximation of $\mathbf{\Sigma}_K$ which is given in Lemma 6 (see Appendix I). Therefore, using the result of Lemma 6 and the fact that $\mathbf{V}$ is unitary, (54) can be simplified as

$$\mathbf{H}^H\mathbf{W}_{RF}\mathbf{W}_{RF}^H\mathbf{H} \approx \left(\frac{\pi N}{4}\right)\mathbf{V}\,\mathbf{V}^H = \left(\frac{\pi N}{4}\right)\mathbf{I}_K. \quad (55)$$

Therefore, from (53) and (55), we get,

$$\mathbf{K}_{\widehat{n}} \approx \left(\frac{4\sigma_n^2}{\pi N}\right)\mathbf{I}_K, \quad (56)$$

and from (20) and (56), we get,

$$\mathbf{K}_{\widehat{n}^*} \approx \left(\frac{4\sigma_n^2}{\pi N}\right)\mathbf{I}_K. \quad (57)$$

Now, substituting the expressions of $\mathbf{K}_{\widehat{n}}$ and $\mathbf{K}_{\widehat{n}^*}$ from (56) and (57) in (18), we get,

$$\mathbf{K}_{\widetilde{n}} = \mathbf{\Phi}_1\mathbf{K}_{\widehat{n}}\mathbf{\Phi}_1^H + \mathbf{G}_1^{-1}\mathbf{G}_2^*\mathbf{\Phi}_1^*\mathbf{K}_{\widehat{n}^*}\mathbf{\Phi}_1^T\mathbf{G}_2^T\mathbf{G}_1^{-H}$$
$$\approx \left(\frac{4\sigma_n^2}{\pi N}\right)\left(\mathbf{\Phi}_1\mathbf{\Phi}_1^H + \mathbf{G}_1^{-1}\mathbf{G}_2^*\mathbf{\Phi}_1^*\mathbf{\Phi}_1^T\mathbf{G}_2^T\mathbf{G}_1^{-H}\right)$$
$$= \left(\frac{4\sigma_n^2}{\pi N}\right)\left(\mathbf{\Phi}_1\mathbf{\Phi}_1^H + \mathbf{G}_1^{-1}\mathbf{G}_2^*\mathbf{\Phi}_1\mathbf{\Phi}_1^H\mathbf{G}_2^T\mathbf{G}_1^{-H}\right)$$
$$= \left(\frac{4\sigma_n^2}{\pi N}\right)\left(\mathbf{I}_K + \mathbf{G}_1^{-1}\mathbf{G}_2^*\mathbf{G}_2^T\mathbf{G}_1^{-H}\right)\mathbf{\Phi}_1\mathbf{\Phi}_1^H$$
$$= \left(\frac{4\sigma_n^2}{\pi N}\right)\left(\mathbf{I}_K + (\mathbf{G}_1^H\mathbf{G}_1)^{-1}\mathbf{G}_2^H\mathbf{G}_2\right)\mathbf{\Phi}_1\mathbf{\Phi}_1^H, \quad (58)$$

where we have used the fact that the diagonal matrices $\mathbf{G}_1$, $\mathbf{G}_2$, and $\mathbf{\Phi}_1$ satisfy $\mathbf{G}_1 = \mathbf{G}_1^T$, $\mathbf{G}_2 = \mathbf{G}_2^T$ and $\mathbf{\Phi}_1 = \mathbf{\Phi}_1^T$ and the product of two diagonal matrices can commute. Also, it is worth noting that $\mathbf{K}_{\widetilde{n}}$ now becomes a diagonal matrix in the large antenna regime. By using the definition of $\mathbf{\Phi}_1$, the term $\mathbf{\Phi}_1\mathbf{\Phi}_1^H$ in (58) can be simplified as

$$\mathbf{\Phi}_1\mathbf{\Phi}_1^H = \left(\mathbf{G}_1 - \mathbf{G}_2^*\mathbf{G}_1^{-*}\mathbf{G}_2\right)^{-1}\left(\mathbf{G}_1 - \mathbf{G}_2^*\mathbf{G}_1^{-*}\mathbf{G}_2\right)^{-H}$$
$$\overset{(a)}{=} \left(\mathbf{G}_1 - \mathbf{G}_2^H\mathbf{G}_1^{-H}\mathbf{G}_2\right)^{-1}\left(\mathbf{G}_1^H - \mathbf{G}_2^H\mathbf{G}_1^{-1}\mathbf{G}_2\right)^{-1}$$
$$= \left[\left(\mathbf{G}_1^H - \mathbf{G}_2^H\mathbf{G}_1^{-1}\mathbf{G}_2\right)\left(\mathbf{G}_1 - \mathbf{G}_2^H\mathbf{G}_1^{-H}\mathbf{G}_2\right)\right]^{-1}$$
$$= \left[\mathbf{G}_1^H\mathbf{G}_1 - 2\mathbf{G}_2^H\mathbf{G}_2 + (\mathbf{G}_2^H\mathbf{G}_2)^2(\mathbf{G}_1^H\mathbf{G}_1)^{-1}\right]^{-1}, \quad (59)$$

where (a) is obtained by using $\mathbf{G}_1 = \mathbf{G}_1^T$ and $\mathbf{G}_2 = \mathbf{G}_2^T$. Hence, after substituting the expression of $\mathbf{\Phi}_1\mathbf{\Phi}_1^H$ from (59) in (58), we get,

$$\mathbf{K}_{\widetilde{n}} = \left(\frac{4\sigma_n^2}{\pi N}\right)\left(\mathbf{I}_K + (\mathbf{G}_1^H\mathbf{G}_1)^{-1}\mathbf{G}_2^H\mathbf{G}_2\right)$$
$$\times\left[\mathbf{G}_1^H\mathbf{G}_1 - 2\mathbf{G}_2^H\mathbf{G}_2 + (\mathbf{G}_2^H\mathbf{G}_2)^2(\mathbf{G}_1^H\mathbf{G}_1)^{-1}\right]^{-1}. \quad (60)$$

Therefore, in the large antenna regime and for the $N_{RF} = K$ scenario, (17) can be simplified as

$$R_{sum,K}^{WC} = \log_2\det\left(\mathbf{I}_K + \rho_u\,\mathbf{K}_{\widetilde{n}}^{-1}\right)$$
$$\approx \log_2\left[\prod_{k=1}^{K}\left(1 + \left(\frac{\rho_u\pi N}{4\sigma_n^2}\right)\left(1 + \frac{|G_{2,k}|^2}{|G_{1,k}|^2}\right)^{-1}\right.\right.$$
$$\left.\left.\times\left(\frac{|G_{1,k}|^4 - 2|G_{1,k}|^2|G_{2,k}|^2 + |G_{2,k}|^4}{|G_{1,k}|^2}\right)\right)\right]$$
$$= \log_2\left[\prod_{k=1}^{K}\left(1 + \left(\frac{\rho_u\pi N}{4\sigma_n^2}\right)\frac{(|G_{1,k}|^2 - |G_{2,k}|^2)^2}{|G_{1,k}|^2 + |G_{2,k}|^2}\right)\right]$$
$$= \sum_{k=1}^{K}\log_2\left(1 + \left(\frac{\rho_u\pi N}{4\sigma_n^2}\right)\frac{(|G_{1,k}|^2 - |G_{2,k}|^2)^2}{|G_{1,k}|^2 + |G_{2,k}|^2}\right), \quad (61)$$

where we have used the large antenna approximation of $\mathbf{K}_{\widetilde{n}}$ from (60), the identity $\det(\mathbf{D}) = \prod_{l=1}^{L}[\mathbf{D}]_{l,l}$, where $\mathbf{D}$ is a diagonal matrix of order L. Next, using the definitions of $G_{1,k}$ and $G_{2,k}$ given in (2), it is easy to verify that

$$|G_{1,k}|^2 - |G_{2,k}|^2 = g_{T,k}\cos\phi_{T,k} \quad (62)$$

and

$$|G_{1,k}|^2 + |G_{2,k}|^2 = \left(\frac{1 + g_{T,k}^2}{2}\right). \quad (63)$$

Finally, from (61), (62) and (63), we get,

$$R_{sum,K}^{WC} \approx \sum_{k=1}^{K}\log_2\left(1 + \left(\frac{\rho_u\pi N}{4\sigma_n^2}\right)\left(\frac{2g_{T,k}^2\cos^2\phi_{T,k}}{1 + g_{T,k}^2}\right)\right), \quad (64)$$

which concludes the proof.

APPENDIX E
PROOF OF LEMMA 4

The problem of representing K left singular vectors of $\mathbf{H}$ as a product of $\mathbf{W}_{RF}$ and $\mathbf{W}_{BB}$ is equivalent to the problem of representing an arbitrary vector $\mathbf{a} \in \mathbb{C}^{N\times 1}$ with $\|\mathbf{a}\|_2 = 1$ as a product of $\mathbf{B} \in \mathbb{C}^{N\times 2}$ and $\mathbf{c} \in \mathbb{C}^{2\times 1}$, i.e., $\mathbf{a} = \mathbf{Bc}$, where $|[\mathbf{B}]_{n,l}| = 1$. This problem has been studied by various researchers in the past, for example, see Theorem 1 of [16], and equations (12) and (13) of [17]. By following the above solutions, we arrive at (33).

APPENDIX F
PROOF OF THEOREM 2

When the hybrid combiner of Lemma 4 is applied, $\mathbf{W}_{RF}\mathbf{W}_{BB}$ simplifies to $\mathbf{U}_{1:K}$ and hence, we get,

$$\mathbf{W}_{BB}^H\mathbf{W}_{RF}^H\mathbf{W}_{RF}\mathbf{W}_{BB} = \mathbf{U}_{1:K}^H\mathbf{U}_{1:K} = \mathbf{I}_K, \tag{65}$$

$$\text{and} \quad \mathbf{W}_{BB}^H\mathbf{W}_{RF}^H\mathbf{H} = \mathbf{U}_{1:K}^H\mathbf{U}\mathbf{\Sigma}\mathbf{V}^H = \mathbf{\Sigma}_K\mathbf{V}^H, \tag{66}$$

where we have used the unitary property of $\mathbf{U}$ and SVD of $\mathbf{H}$. After substituting the expressions of $\mathbf{W}_{BB}^H\mathbf{W}_{RF}^H\mathbf{W}_{RF}\mathbf{W}_{BB}$ and $\mathbf{W}_{BB}^H\mathbf{W}_{RF}^H\mathbf{H}$ from (65) and (66) in (19), we get,

$$\begin{aligned}\mathbf{K}_{\widehat{n}} &= \sigma_n^2(\mathbf{W}_{BB}^H\mathbf{W}_{RF}^H\mathbf{H})^{-1}\mathbf{W}_{BB}^H\mathbf{W}_{RF}^H \\ &\quad\times \mathbf{W}_{RF}\mathbf{W}_{BB}(\mathbf{W}_{BB}^H\mathbf{W}_{RF}^H\mathbf{H})^{-H} \\ &= \sigma_n^2(\mathbf{\Sigma}_K\mathbf{V}^H)^{-1}(\mathbf{\Sigma}_K\mathbf{V}^H)^{-H} \\ &= \sigma_n^2(\mathbf{V}\,\mathbf{\Sigma}_K^H\mathbf{\Sigma}_K\mathbf{V}^H)^{-1} \\ &\approx \left(\frac{\sigma_n^2}{N}\right)(\mathbf{V}\mathbf{V}^H)^{-1} = \left(\frac{\sigma_n^2}{N}\right)\mathbf{I}_K,\end{aligned} \tag{67}$$

where we have used the result of Lemma 6 to obtain (67). It is important to note that the approximation in (67) is valid only for the large antenna regime whereas the hybrid combiner of Lemma 4 is optimal for all values of N. Therefore, from (18), (20), and (67), we get,

$$\begin{aligned}\mathbf{K}_{\widetilde{n}} &= \mathbf{\Phi}_1\mathbf{K}_{\widehat{n}}\mathbf{\Phi}_1^H + \mathbf{G}_1^{-1}\mathbf{G}_2^*\mathbf{\Phi}_1^*\mathbf{K}_{\widehat{n}^*}\mathbf{\Phi}_1^T\mathbf{G}_2^T\mathbf{G}_1^{-H} \\ &\approx \left(\frac{\sigma_n^2}{N}\right)(\mathbf{\Phi}_1\mathbf{\Phi}_1^H + \mathbf{G}_1^{-1}\mathbf{G}_2^*\mathbf{\Phi}_1^*\mathbf{\Phi}_1^T\mathbf{G}_2^T\mathbf{G}_1^{-H}) \\ &= \left(\frac{\sigma_n^2}{N}\right)\left(\mathbf{I}_K + (\mathbf{G}_1^H\mathbf{G}_1)^{-1}\mathbf{G}_2^H\mathbf{G}_2\right)\mathbf{\Phi}_1\mathbf{\Phi}_1^H \\ &= \left(\frac{\sigma_n^2}{N}\right)\left(\mathbf{I}_K + (\mathbf{G}_1^H\mathbf{G}_1)^{-1}\mathbf{G}_2^H\mathbf{G}_2\right) \\ &\quad\times\left[\mathbf{G}_1^H\mathbf{G}_1 - 2\mathbf{G}_2^H\mathbf{G}_2 + (\mathbf{G}_2^H\mathbf{G}_2)^2(\mathbf{G}_1^H\mathbf{G}_1)^{-1}\right]^{-1},\end{aligned} \tag{68}$$

where we have used the simplification of $\mathbf{\Phi}_1\mathbf{\Phi}_1^H$ from (59) (as, $\mathbf{\Phi}_1 = \left(\mathbf{G}_1 - \mathbf{G}_2^*\mathbf{G}_1^{-*}\mathbf{G}_2\right)^{-1}$ is independent of N_{RF} which implies that $\mathbf{\Phi}_1\mathbf{\Phi}_1^H$ will remain same for all values of N_{RF}). We also observe that the structure of $\mathbf{K}_{\widetilde{n}}$ for the $N_{RF} = 2K$ scenario (see (68)) is similar to that for $N_{RF} = K$ scenario (see (60)) except for a factor of $(4/\pi)$. Therefore, the remaining proof of Theorem 2 can be directly obtained by following (60)-(64), but after ignoring the factor of $(4/\pi)$. Hence, for the large antenna regime and $N_{RF} = 2K$ scenario, (17) can be simplified as

$$\begin{aligned}R_{sum,2K}^{WC} &= \log_2\det\left(\mathbf{I}_K + \rho_u\,\mathbf{K}_{\widetilde{n}}^{-1}\right) \\ &\approx \sum_{k=1}^{K}\log_2\left(1 + \left(\frac{\rho_u N}{\sigma_n^2}\right)\left(\frac{2g_{T,k}^2\cos^2\phi_{T,k}}{1+g_{T,k}^2}\right)\right),\end{aligned} \tag{69}$$

which completes the proof.

APPENDIX G
PROOF OF LEMMA 5

For the $K \le N_{RF} \le 2K$ scenario, the N_{RF} RF chains are divided into two groups: (i) $2(N_{RF} - K)$ RF chains, (ii) $(2K - N_{RF})$ RF chains. From Lemma 4, it is clear that if the number of available RF chains is twice the number of UEs, then an FD combiner can be realized. Therefore, for the $(N_{RF} - K)$ UEs, an FD combiner is derived by using Lemma 4 and $2(N_{RF} - K)$ RF chains whereas for the remaining $(2K - N_{RF})$ UEs, a hybrid combiner is derived by using Lemma 2 and $(2K - N_{RF})$ RF chains.

APPENDIX H
PROOF OF THEOREM 3

It is clear from Lemma 5 that for the $K \le N_{RF} \le 2K$ scenario, the first $2(N_{RF} - K)$ RF chains (2 RF chains for each UE) are used to realize an FD combiner to serve $(N_{RF} - K)$ UEs whereas the remaining $(2K - N_{RF})$ RF chains (1 RF chain for each UE) are used to realize a hybrid combiner to serve the remaining $(2K - N_{RF})$ UEs. Hence, the UL achievable sum-rate for the first $(N_{RF} - K)$ UEs can be directly derived by using Theorem 2 whereas the UL achievable sum-rate for the remaining $(2K - N_{RF})$ UEs can be derived by using Theorem 1. Therefore, the total UL achievable sum-rate for K UEs is obtained by adding the sum-rates of $(N_{RF} - K)$ UEs and $(2K - N_{RF})$ UEs, which concludes the proof.

APPENDIX I
STATEMENT AND PROOF OF LEMMA 6

Lemma 6: If the channel matrix $\mathbf{H} \in \mathbb{C}^{N\times K}$ *is i.i.d. Rayleigh faded, then in the large antenna regime, the diagonal* $K \times K$ *matrix* $\mathbf{\Sigma}_K$ *containing the singular values of* $\mathbf{H}$ *can be approximated as*

$$\mathbf{\Sigma}_K \approx \sqrt{N}\mathbf{I}_K. \tag{70}$$

Proof: It is well known that when $[\mathbf{H}]_{n,k} \sim \mathcal{CN}(0,1)$, $\lim_{N\to\infty}\sigma_{max}^2/N = \lim_{N\to\infty}\sigma_{min}^2/N = 1$, where σ_{max} and σ_{min} are, respectively, the largest and the smallest singular values of $\mathbf{H}$ (see Sec. 7.1.4 of [48] for more details). Hence, the condition number of $\mathbf{H}$, i.e., $\sigma_{max}/\sigma_{min} \approx 1$ in the large antenna regime, which implies that all the singular values of $\mathbf{H}$ are approximately equal, i.e., $\mathbf{\Sigma}_K \approx \sigma\mathbf{I}_K$. To find the value of σ, we have $||\mathbf{H}||_F^2 = \text{Tr}(\mathbf{H}^H\mathbf{H}) = \text{Tr}(\mathbf{V}\mathbf{\Sigma}^H\mathbf{U}^H\mathbf{U}\mathbf{\Sigma}\mathbf{V}^H) = \text{Tr}(\mathbf{V}\mathbf{\Sigma}^H\mathbf{\Sigma}\mathbf{V}^H) = \text{Tr}(\mathbf{V}^H\mathbf{V}\mathbf{\Sigma}^H\mathbf{\Sigma}) = \text{Tr}(\mathbf{\Sigma}^H\mathbf{\Sigma}) = K\sigma^2$, where we have used the identity $\text{Tr}(\mathbf{AB}) = \text{Tr}(\mathbf{BA})$. Therefore, we get $\sigma = ||\mathbf{H}||_F/\sqrt{K}$.

Next, due to channel hardening observed in an i.i.d. Rayleigh fading environment, $\lim_{N\to\infty} ||\mathbf{h}_k||^2/\mathbb{E}[||\mathbf{h}_k||^2] = 1 \ \forall \ k$ which implies that for large antenna arrays, $||\mathbf{H}||_F \approx \mathbb{E}[||\mathbf{H}||_F] = \sqrt{NK}$ (see Sec. 2.5.1, [53]). Hence, using the above result, we get $\sigma \approx \sqrt{N}$ in the large antenna regime, which concludes the proof. ■

REFERENCES

[1] E. Telatar, "Capacity of multi-antenna Gaussian channels," *Eur. Trans. Telecommun.*, vol. 10, no. 6, pp. 585–596, Nov. 1999.

[2] A. Goldsmith, S. A. Jafar, N. Jindal, and S. Vishwanath, "Capacity limits of MIMO channels," *IEEE J. Sel. Areas Commun.*, vol. 21, no. 5, pp. 684–702, Jun. 2003.

[3] P. Viswanath and D. N. C. Tse, "Sum capacity of the vector Gaussian broadcast channel and uplink–downlink duality," *IEEE Trans. Inf. Theory*, vol. 49, no. 8, pp. 1912–1921, Aug. 2003.

[4] T. L. Marzetta, "Noncooperative cellular wireless with unlimited numbers of base station antennas," *IEEE Trans. Wireless Commun.*, vol. 9, no. 11, pp. 3590–3600, Nov. 2010.

[5] F. Rusek, D. Persson, B. K. Lau, E. G. Larsson, T. L. Marzetta, and F. Tufvesson, "Scaling up MIMO: Opportunities and challenges with very large arrays," *IEEE Signal Process. Mag.*, vol. 30, no. 1, pp. 40–60, Jan. 2013.

[6] H. Q. Ngo, E. G. Larsson, and T. L. Marzetta, "Energy and spectral efficiency of very large multiuser MIMO systems," *IEEE Trans. Commun.*, vol. 61, no. 4, pp. 1436–1449, Apr. 2013.

[7] K. Xu, Z. Shen, Y. Wang, X. Xia, and D. Zhang, "Hybrid time-switching and power splitting SWIPT for full-duplex massive MIMO systems: A beam-domain approach," *IEEE Trans. Veh. Technol.*, vol. 67, no. 8, pp. 7257–7274, Aug. 2018.

[8] Z. Shen, K. Xu, X. Xia, W. Xie, and D. Zhang, "Spatial sparsity based secure transmission strategy for massive MIMO systems against simultaneous jamming and eavesdropping," *IEEE Trans. Inf. Forensics Security*, vol. 15, pp. 3760–3774, 2020.

[9] Z. Shen, K. Xu, and X. Xia, "Beam-domain anti-jamming transmission for downlink massive MIMO systems: A Stackelberg game perspective," *IEEE Trans. Inf. Forensics Security*, vol. 16, pp. 2727–2742, 2021.

[10] L. C. Godara, "Application of antenna arrays to mobile communications. II. Beam-forming and direction-of-arrival considerations," *Proc. IEEE*, vol. 85, no. 8, pp. 1195–1245, Aug. 1997.

[11] I. Ahmed, H. Khammari, A. Shahid, A. Musa, K. S. Kim, E. De Poorter, and I. Moerman, "A survey on hybrid beamforming techniques in 5G: Architecture and system model perspectives," *IEEE Commun. Surveys Tuts.*, vol. 20, no. 4, pp. 3060–3097, 4th Quart., 2018.

[12] A. F. Molisch, V. V. Ratnam, S. Han, Z. Li, S. L. H. Nguyen, L. Li, and K. Haneda, "Hybrid beamforming for massive MIMO: A survey," *IEEE Commun. Mag.*, vol. 55, no. 9, pp. 134–141, Sep. 2017.

[13] O. A. Ayach, S. Rajagopal, S. A. Surra, Z. Pi, and R. W. Heath, Jr., "Spatially sparse precoding in millimeter wave MIMO systems," *IEEE Trans. Wireless Commun.*, vol. 13, no. 3, pp. 1499–1512, Mar. 2014.

[14] W. Ni, X. Dong, and W.-S. Lu, "Near-optimal hybrid processing for massive MIMO systems via matrix decomposition," *IEEE Trans. Signal Process.*, vol. 65, no. 15, pp. 3922–3933, Aug. 2017.

[15] S. Payami, M. Shariat, M. Ghoraishi, and M. Dianati, "Effective RF codebook design and channel estimation for millimeter wave communication systems," in *Proc. IEEE Int. Conf. Commun. Workshop (ICCW)*, Jun. 2015, pp. 1226–1231.

[16] X. Zhang, A. F. Molisch, and S.-Y. Kung, "Variable-phase-shift-based RF-baseband codesign for MIMO antenna selection," *IEEE Trans. Signal Process.*, vol. 53, no. 11, pp. 4091–4103, Nov. 2005.

[17] S. Payami, M. Ghoraishi, and M. Dianati, "Hybrid beamforming for large antenna arrays with phase shifter selection," *IEEE Trans. Wireless Commun.*, vol. 15, no. 11, pp. 7258–7271, Nov. 2016.

[18] F. Sohrabi and W. Yu, "Hybrid digital and analog beamforming design for large-scale antenna arrays," *IEEE J. Sel. Topics Signal Process.*, vol. 10, no. 3, pp. 501–513, Apr. 2016.

[19] X. Wu, D. Liu, and F. Yin, "Hybrid beamforming for multi-user massive MIMO systems," *IEEE Trans. Commun.*, vol. 66, no. 9, pp. 3879–3891, Sep. 2018.

[20] W. Tan, D. Xie, J. Xia, W. Tan, L. Fan, and S. Jin, "Spectral and energy efficiency of massive MIMO for hybrid architectures based on phase shifters," *IEEE Access*, vol. 6, pp. 11751–11759, 2018.

[21] S. Payami, N. M. Balasubramanya, C. Masouros, and M. Sellathurai, "Phase shifters versus switches: An energy efficiency perspective on hybrid beamforming," *IEEE Wireless Commun. Lett.*, vol. 8, no. 1, pp. 13–16, Feb. 2019.

[22] A. Alkhateeb, Y.-H. Nam, J. Zhang, and R. W. Heath, Jr., "Massive MIMO combining with switches," *IEEE Wireless Commun. Lett.*, vol. 5, no. 3, pp. 232–235, Jun. 2016.

[23] V. Venkateswaran and A.-J. van der Veen, "Analog beamforming in MIMO communications with phase shift networks and online channel estimation," *IEEE Trans. Signal Process.*, vol. 58, no. 8, pp. 4131–4143, Aug. 2010.

[24] S. Payami, M. Ghoraishi, M. Dianati, and M. Sellathurai, "Hybrid beamforming with a reduced number of phase shifters for massive MIMO systems," *IEEE Trans. Veh. Technol.*, vol. 67, no. 6, pp. 4843–4851, Jun. 2018.

[25] K. Xu, Z. Shen, Y. Wang, and X. Xia, "Location-aided mMIMO channel tracking and hybrid beamforming for high-speed railway communications: An angle-domain approach," *IEEE Syst. J.*, vol. 14, no. 1, pp. 93–104, Mar. 2020.

[26] T. E. Bogale, L. B. Le, and X. Wang, "Hybrid analog-digital channel estimation and beamforming: Training-throughput tradeoff," *IEEE Trans. Commun.*, vol. 63, no. 12, pp. 5235–5249, Dec. 2015.

[27] Y.-C. Ko and M.-J. Kim, "Channel estimation and analog beam selection for uplink multiuser hybrid beamforming system," *EURASIP J. Wireless Commun. Netw.*, vol. 2016, no. 1, p. 155, Jul. 2016.

[28] D. Mishra and H. Johansson, "Efficacy of hybrid energy beamforming with phase shifter impairments and channel estimation errors," *IEEE Signal Process. Lett.*, vol. 26, no. 1, pp. 99–103, Jan. 2019.

[29] X. Yang, M. Matthaiou, J. Yang, C.-K. Wen, F. Gao, and S. Jin, "Hardware-constrained millimeter-wave systems for 5G: Challenges, opportunities, and solutions," *IEEE Commun. Mag.*, vol. 57, no. 1, pp. 44–50, Jan. 2019.

[30] T. Schenk, *RF Imperfections in High-Rate Wireless Systems: Impact and Digital Compensation*. Dordrecht, The Netherlands: Springer, 2008.

[31] J. Qi and S. Aissa, "Analysis and compensation of I/Q imbalance in MIMO transmit-receive diversity systems," *IEEE Trans. Commun.*, vol. 58, no. 5, pp. 1546–1556, May 2010.

[32] N. Kolomvakis, M. Matthaiou, and M. Coldrey, "IQ imbalance in multiuser systems: Channel estimation and compensation," *IEEE Trans. Commun.*, vol. 64, no. 7, pp. 3039–3051, Jul. 2016.

[33] S. Zarei, W. H. Gerstacker, J. Aulin, and R. Schober, "I/Q imbalance aware widely-linear receiver for uplink multi-cell massive MIMO systems: Design and sum rate analysis," *IEEE Trans. Wireless Commun.*, vol. 15, no. 5, pp. 3393–3408, May 2016.

[34] W. Zhang, R. C. de Lamare, C. Pan, M. Chen, J. Dai, B. Wu, and X. Bao, "Widely linear precoding for large-scale MIMO with IQI: Algorithms and performance analysis," *IEEE Trans. Wireless Commun.*, vol. 16, no. 5, pp. 3298–3312, May 2017.

[35] S. Wang and L. Zhang, "Signal processing in massive MIMO with IQ imbalances and low-resolution ADCs," *IEEE Trans. Wireless Commun.*, vol. 15, no. 12, pp. 8298–8312, Dec. 2016.

[36] R. Mahendra, S. K. Mohammed, and R. K. Mallik, "Performance of MRC and ZF receivers in IQ-impaired uplink massive MIMO systems," in *Proc. Int. Conf. Commun. Syst. Netw. (COMSNETS)*, Bengaluru, India, Jan. 2021, pp. 202–206.

[37] N. Kolomvakis, M. Coldrey, T. Eriksson, and M. Viberg, "Massive MIMO systems with IQ imbalance: Channel estimation and sum rate limits," *IEEE Trans. Commun.*, vol. 65, no. 6, pp. 2382–2396, Jun. 2017.

[38] Y. Xiong, N. Wei, and Z. Zhang, "An LMMSE-based receiver for uplink massive MIMO systems with randomized IQ imbalance," *IEEE Commun. Lett.*, vol. 22, no. 8, pp. 1624–1627, Aug. 2018.

[39] J. Jee, G. Kwon, and H. Park, "Regularized zero-forcing precoder for massive MIMO system with transceiver I/Q imbalances," *IEEE Wireless Commun. Lett.*, vol. 8, no. 4, pp. 1028–1031, Aug. 2019.

[40] S. Teodoro, A. Silva, R. Dinis, F. M. Barradas, P. M. Cabral, and A. Gameiro, "Theoretical analysis of nonlinear amplification effects in massive MIMO systems," *IEEE Access*, vol. 7, pp. 172277–172289, 2019.

[41] N. N. Moghadam, G. Fodor, M. Bengtsson, and D. J. Love, "On the energy efficiency of MIMO hybrid beamforming for millimeter-wave systems with nonlinear power amplifiers," *IEEE Trans. Wireless Commun.*, vol. 17, no. 11, pp. 7208–7221, Nov. 2018.

[42] A. K. Papazafeiropoulos, G. K. Papageorgiou, O. Y. Kolawole, P. Kourtessis, S. Chatzinotas, J. M. Senior, M. Sellathurai, and T. Ratnarajah, "Towards the assessment of realistic hybrid precoding in millimeter wave MIMO systems with hardware impairments," *IET Commun.*, pp. 1–14, Apr. 2021.
[43] I. Ahmed, H. Khammari, and F. Alraddady, "A low complexity hybrid combiner design for the ill-conditioned multiuser mmWave massive MIMO uplink," *IET Commun.*, pp. 1–12, Mar. 2021.
[44] S. Ghosh and R. Chopra, "Downlink pilots for hybrid massive MIMO under reciprocity imperfections," *IEEE Commun. Lett.*, vol. 24, no. 10, pp. 2334–2338, Oct. 2020.
[45] N. Zhang, H. Yin, and W. Wang, "Hybrid beamforming for millimetre wave massive MU-MIMO systems with IQ imbalance," *IET Commun.*, vol. 13, no. 6, pp. 776–785, Apr. 2019.
[46] R. Mahendra, S. K. Mohammed, and R. K. Mallik, "Compensation of receiver IQ imbalance in mm-wave hybrid beamforming systems," in *Proc. IEEE 92nd Veh. Technol. Conf. (VTC-Fall)*, Victoria, BC, Canada, Nov. 2020, pp. 1–6.
[47] R. Mahendra, S. K. Mohammed, and R. K. Mallik, "Transmitter IQ imbalance pre-compensation for mm-wave hybrid beamforming systems," in *Proc. IEEE 91st Veh. Technol. Conf. (VTC-Spring)*, Antwerp, Belgium, May 2020, pp. 1–7.
[48] T. Marzetta, E. Larsson, H. Yang, and H. Ngo, *Fundamentals of Massive MIMO*. Cambridge, U.K.: Cambridge Univ. Press, 2016.
[49] A. E. Gamal and Y. H. Kim, *Network Information Theory*. Cambridge, U.K.: Cambridge Univ. Press, 2011.
[50] R. A. Horn and C. R. Johnson, *Matrix Analysis*, 2nd ed. Cambridge, U.K.: Cambridge Univ. Press, 2013.
[51] R. K. Mallik, "The exponential correlation matrix: Eigen-analysis and applications," *IEEE Trans. Wireless Commun.*, vol. 17, no. 7, pp. 4690–4705, Jul. 2018.
[52] S. L. Loyka, "Channel capacity of MIMO architecture using the exponential correlation matrix," *IEEE Commun. Lett.*, vol. 5, no. 9, pp. 369–371, Sep. 2001.
[53] E. Björnson, J. Hoydis, and L. Sanguinetti, "Massive MIMO networks: Spectral, energy, and hardware efficiency," *Found. Trends Signal Process.*, vol. 11, nos. 3–4, pp. 154–655, 2017.

RACHIT MAHENDRA (Graduate Student Member, IEEE) received the AMIETE degree (Hons.) in electronics and telecommunication engineering from The Institution of Electronics and Telecommunication Engineers (IETE), New Delhi, India, in 2010, and the M.Tech. degree in signal processing from the Netaji Subhas Institute of Technology (NSIT), University of Delhi, New Delhi, in 2014. He is currently pursuing the Ph.D. degree in electrical engineering with the Indian Institute of Technology Delhi (IIT Delhi), New Delhi. Earlier, he was working as an Assistant Professor with the Department of Electronics and Communication Engineering, JRE Group of Institutions, Greater Noida, Uttar Pradesh, India, affiliated to Dr. A. P. J. Abdul Kalam Technical University, Lucknow, Uttar Pradesh. His research interests include digital compensation of hardware impairments in wireless communication systems with main focus on large antenna array (massive MIMO) systems and hybrid beamforming systems. He was a recipient of the Smt. Radhabai Kapre Gold Medal Award 2011, which is given for securing highest CGPA and completing AMIETE in four years without exemption.

SAIF KHAN MOHAMMED (Senior Member, IEEE) received the B.Tech. degree in computer science and engineering from the Indian Institute of Technology Delhi (IIT Delhi), New Delhi, India, in 1998, and the Ph.D. degree from the Electrical and Communication Engineering Department, Indian Institute of Science, Bengaluru, India, in 2010. From 2000 to 2003, he was with Ishoni Networks, Inc., Santa Clara, CA, USA, as a Senior Chip Architecture Engineer. He was a Systems and Algorithm Designer with the Wireless Systems Group, Texas Instruments , Bengaluru, from 2003 to 2007. From 2010 to 2011, he was a Postdoctoral Researcher at the Communication Systems Division (Commsys), Electrical Engineering Department (ISY), Linköping University, Sweden. He was an Assistant Professor at Commsys, from September 2011 to February 2013. He is currently an Associate Professor with the Department of Electrical Engineering, IIT Delhi. He holds four granted U.S. patents in multi-user detection and precoding for multiple-input multiple-output (MIMO) communication systems. His research interests include wireless communication using large antenna arrays, coding, and signal processing for wireless communication systems, information theory, and statistical signal processing. He is a fellow of the Institution of Electronics and Telecommunication Engineers, India. He received the 2017 NASI Scopus Young Scientist Award and the Teaching Excellence Award at IIT Delhi, for the year 2016–2017. He was also a recipient of the Visvesvaraya Young Faculty Fellowship from the Ministry of Electronics and IT, Government of India, from 2016 to 2019, and the Young Indian Researcher Fellowship from the Italian Ministry of University and Research (MIUR), from 2009 to 2010. He holds the Prof. Kishan and Pramila Gupta Chair at IIT Delhi. He has served as an Editor for IEEE Wireless Communications Letters and *Physical Communication* journal (Elsevier), and currently serves as an Editor for IEEE Transactions on Wireless Communications.

RANJAN K. MALLIK (Fellow, IEEE) received the B.Tech. degree from the Indian Institute of Technology Kanpur, Kanpur, in 1987, and the M.S. and Ph.D. degrees from the University of Southern California, Los Angeles, in 1988 and 1992, respectively, all in electrical engineering.

From August 1992 to November 1994, he was a Scientist with the Defence Electronics Research Laboratory, Hyderabad, India, working on missile and EW projects. From November 1994 to January 1996, he was a Faculty Member with the Department of Electronics and Electrical Communication Engineering, Indian Institute of Technology Kharagpur, Kharagpur. From January 1996 to December 1998, he was with the Faculty of the Department of Electronics and Communication Engineering, Indian Institute of Technology Guwahati, Guwahati. Since December 1998, he has been with the Faculty of the Department of Electrical Engineering, Indian Institute of Technology Delhi, New Delhi, where he is currently an Institute Chair Professor. His research interests include diversity combining and channel modeling for wireless communications, space-time systems, cooperative communications, multiple-access systems, power line communications, molecular communications, difference equations, and linear algebra. He is a member of Eta Kappa Nu, the IEEE Communications, Information Theory, and Vehicular Technology Societies, the American Mathematical Society, and the International Linear Algebra Society; a fellow of the Indian National Academy of Engineering, the Indian National Science Academy, The National Academy of Sciences, Prayagraj, India, the Indian Academy of Sciences, Bengaluru, The World Academy of Sciences-for the advancement of science in developing countries (TWAS), The Institution of Engineering and Technology, U.K., The Institution of Electronics and Telecommunication Engineers, India, and The Institution of Engineers (India); and a Life Member of the Indian Society for Technical Education. He was a recipient of the Hari Om Ashram Prerit Dr. Vikram Sarabhai Research Award in the field of electronics, telematics, informatics, and automation; the Shanti Swarup Bhatnagar Prize in engineering sciences; the Khosla National Award; and the J. C. Bose Fellowship. He has served as an Area Editor and an Editor for the IEEE Transactions on Wireless Communications, and as an Editor for the IEEE Transactions on Communications.